


Review

Utilization of Deep Eutectic Solvents to Reduce the Release of Hazardous Gases to the Atmosphere: A Critical Review

Irfan Wazeer¹, Mohamed K. Hadj-Kali^{1,*} and Inas M. Al-Nashef² 

¹ Chemical Engineering Department, King Saud University, P.O. Box 800, Riyadh 11421, Saudi Arabia; iwazeer@ksu.edu.sa

² Department of Chemical Engineering, Masdar Institute, Khalifa University of Science and Technology, P.O. Box 54224, Abu Dhabi, UAE; enas.nashef@ku.ac.ae

* Correspondence: mhadjkali@ksu.edu.sa

Abstract: The release of certain gases to the atmosphere is controlled in many countries owing to their negative impact on the environment and human health. These gases include carbon dioxide (CO₂), sulfur oxides (SO_x), nitrogen oxides (NO_x), hydrogen sulfide (H₂S) and ammonia (NH₃). Considering the major contribution of greenhouse gases to global warming and climate change, mitigation of these gases is one of the world's primary challenges. Nevertheless, the commercial processes used to capture these gases suffer from several drawbacks, including the use of volatile solvents, generation of hazardous byproducts, and high-energy demand. Research in green chemistry has resulted in the synthesis of potentially green solvents that are non-toxic, efficient, and environmentally friendly. Deep eutectic solvents (DESs) are novel solvents that upon wise choice of their constituents can be green and tunable with high biocompatibility, high degradability, and low cost. Consequently, the capture of toxic gases by DESs is promising and environmentally friendly and has attracted much attention during the last decade. Here, we review recent results on capture of these gases using different types of DESs. The effect of different parameters, such as chemical structure, molar ratio, temperature, and pressure, on capture efficiency is discussed.

Keywords: deep eutectic solvents; climate change; human health; CO₂ capture; toxic gases; desulfurization; denitrogenation



Citation: Wazeer, I.; Hadj-Kali, M.K.; Al-Nashef, I.M. Utilization of Deep Eutectic Solvents to Reduce the Release of Hazardous Gases to the Atmosphere: A Critical Review. *Molecules* **2021**, *26*, 75. <https://doi.org/10.3390/molecules26010075>

Received: 5 December 2020

Accepted: 23 December 2020

Published: 26 December 2020

Publisher's Note: MDPI stays neutral with regard to jurisdictional claims in published maps and institutional affiliations.



Copyright: © 2020 by the authors. Licensee MDPI, Basel, Switzerland. This article is an open access article distributed under the terms and conditions of the Creative Commons Attribution (CC BY) license (<https://creativecommons.org/licenses/by/4.0/>).

1. Introduction

Climate change is an exceedingly critical environmental challenge, and its mitigation and remediation have gained widespread attention. Many countries around the world, have instituted laws and regulations to maintain environmental air quality and control the emission of pollutants that harm human health and affect the atmosphere [1]. Six major air contaminants have been identified based on National Ambient Air Quality Standards, including ozone, particulate matter, carbon monoxide, sulfur oxides (SO_x), nitrogen oxides (NO_x), and lead. Long-term exposure to these contaminants has been shown to have a harmful impact on human wellness over decades, evincing in a broad range of problems, including higher infant mortality rates and inherited respiratory diseases [2]. SO_x and NO_x, in particular, have serious effects on multiple human organs, damaging the nervous, respiratory, gastrointestinal, and cardiovascular systems to a degree that has been proven to be lethal. When gases such as SO_x and NO_x are transformed via chemical reactions, a portion of particulate matter is produced in the air. In the presence of sunlight, ozone is formed by chemical reactions between volatile organic compounds (VOCs) and NO_x. Both SO_x and NO_x have harmful effects, in addition to their severe impacts on human health and climate, because they generate other air pollutants. A fossil-fuel driven plant releases approximately 80% of the NO_x and 70% of the SO_x present in the surrounding atmosphere, making oxide mitigation and elimination a critical task in automotive and industrial processes [3].

In the petrochemical industry, fuel is a primary source of pollutants in the environment, as it is rich in aromatics, nitrogen and sulfur-containing aromatic substances that are burned to create harmful contaminants. Thus, both the climate and human health can be influenced by the composition of fossil fuel oils [4]. Strict environmental standards to eliminate aromatics and sulfur- and nitrogen-containing fuel oil content have been implemented around the world to improve air quality. In short, harmful emissions are to be restricted by the generation of clean-burn fuel oils. In addition, the aromatic products of sulfur and nitrogen are troublesome in the refining of oil and gas because they are the sources of catalytic toxicity or deactivation, degradation and gum formation. High levels of aromatic content have been shown to affect the quality of the fuel; it is therefore important that aromatic compounds be separated from aliphatic ones [5]. Currently, hydrodesulfurization (HDS) is a proven desulfurization process that is widely used in the industry [6]. Aliphatic hydrocarbon sulfur content can be efficiently eliminated by HDS. However, because of their broad steric hindrance, it is difficult for polycyclic organic sulfides such as thiophene, benzothiophene, dibenzothiophene, and their derivatives to attain deep removal. Even if deep desulfurization can be accomplished, operating conditions are excessively harsh, resulting in a significant increase in the cost of desulfurization. Inhibition of the HDS process by the presence of nitrogen-containing compounds that poison the catalysts has also stimulated the need for denitrogenation. Hydrodenitrogenation is the most prominent denitrogenation process in the industry, but it involves harsh working conditions, and significant hydrogen consumption and capital costs. Furthermore, it is difficult to reach high denitrogenation efficiency [7]. The nitrogen content limit in diesel fuel has been regulated in many countries since 2011, and the allowed concentration was lowered from 70 ppm to <0.10 ppm. Comparably, in most countries, the sulfur content has been set to as low as 10 ppm (on an annual average basis) [8].

The rise in global temperatures constitutes an emergent risk to the earth, with an estimated 2 °C rise predicted by the end of this century [9]. The phenomenon of a gradual rise of average global temperature is known as the greenhouse effect and can be attributed to a group of greenhouse gases, of which carbon dioxide (CO₂) is the most dominant [10]. A direct cause of climate change is the steady annual growth of CO₂, which is responsible for over 70% of the world's estimated greenhouse gases. Additionally, CO₂ has direct adverse health consequences on human health, with signs varying from acute breathlessness to lack of cognitive capacity, based on the degree and length of exposure to CO₂. Such symptoms can be acute or chronic and can have a detrimental impact on human health if excessive CO₂ exists in indoor and outdoor air [11].

Various processes have been developed for the removal of toxic gases, including adsorption, absorption, and membrane separation [12,13]. Amine scrubbing is the most prominent among chemical absorption methods [14]. The most widely used amine solvents for CO₂ removal are monoethanolamine (MEA), diethanolamine (DEA), triethanolamine (TEA), diglycolamine (DGA), and methyldiethanolamine (MDEA). However, major downsides of amine scrubbing methods include the degradation of amines, the corrosion caused by the components produced during amine reactions with CO₂ and high regeneration energy (Figure 1) [15–17]. Other good CO₂ absorbents include caustic solvents such as calcium hydroxide, potassium hydroxide, and sodium hydroxide [18]. Unfortunately, the regeneration of solvents remains a big concern. Carbonate solutions have also been employed for the absorption of acidic gases. While carbonate solutions have low volatility and result in a lower corrosion rate, they have major drawbacks in terms of lower absorption rates in comparison with caustic and amine solutions [19]. Compared to caustic and amine solutions, amino acid salt solutions have the benefit of improved regeneration owing to their lower volatility. However, the high molecular weight of amino acid salt solutions is a major drawback and increases the capital expenses of the absorber [20]. Owing to its simplicity of design, energy efficiency, and ease of scale-up, the use of membrane technology to capture CO₂ has seen rapid growth in popularity. Unfortunately, most membranes require regular replacement because they do not last long in practical industrial environments [21].



Figure 1. Major challenges of using amine solutions [15–17].

In recent decades, medicinal, chemical, and industrial processes have widely utilized solvents accounting for nearly 30% of emissions of VOCs and 60% of industrial emissions worldwide [22]. Green processes in all areas of chemistry and engineering have drawn significant attention over the past 20 years, representing an increasing desire to minimize the usage of hazardous and unsafe chemicals and to raise understanding of environmental concerns. Green chemistry and engineering is also responsible for limiting or eliminating the usage of harmful and hazardous chemicals and for designing ecologically sustainable chemical procedures [23]. Solvents comprise a significant field of research in green chemistry with most of the traditional chemicals being toxic and flammable. Therefore, researchers have established many safer alternatives, such as water-based or solvent-free systems, ionic liquids (ILs), and supercritical fluids (SCF), with the solvent-free system representing the best-case scenario [24,25]. However, the use of solvents cannot always be eliminated because of their pivotal role in heat and mass transfer, and dissolution and separation operations [26]. For example, water, the world's most abundant compound, has already been used in a number of chemical processes as a solvent. Even so, the drawbacks of using water as a solvent include the negligible solubility of various organic compounds and the possibility of contamination, with a further downside posed by the high vaporization energy of this solvent. Another solution is to substitute typically organic solvents with SCFs; that are chemically stable, easy to handle, and safe. However, owing to their non-polar existence, SCFs still have some drawbacks, e.g., CO₂ has minimal dissolving capacity for polar solutes [27].

Since the early 2000s, ILs, a form of newly synthesized solvents, have garnered a great deal of attention from the research community in multidisciplinary fields. ILs are molten salts, composed of ions, with a melting point below 100 °C [28,29]. The main aspects of ILs over conventional organic solvents are their minimal vapor pressure, good thermal characteristics, wide liquid range, miscibility, solubility range, and chemical reaction suitability. Nevertheless, studies indicated that the 'green' characteristics of ILs are at least questionable because of the known drawbacks of these solvents; for example, high preparation costs, high viscosity, equivalent or higher toxicity, and poor biodegradability compared to organic solvents [30,31].

Deep eutectic solvents (DESs) have become attractive replacements for traditional solvents and ILs in order to tackle the high levels of toxicity and costs of ILs. However, the definition of DESs remains controversial, and different definitions do not discriminate DESs from other mixtures, as all mixtures of immiscible solids are eutectic and various compounds may form hydrogen bonds when mixed [32]. The concept of DESs as a new

class of sustainable solvent was first coined by Abbott et al., and identified as solvents with melting points significantly lower than those of individual components when combined in a proper molar ratio [33]. DESs consist of large, nonsymmetric ions with low lattice energy and thus low melting points and are usually produced by the mixing of a metal salt or hydrogen bond donor (HBD) and a quaternary ammonium salt. The delocalization of charges between HBD and, for example, a halide ion via hydrogen bonding allows the melting points of the mixture to decrease in comparison with the melting points of the individual constituents. Recently, Martins et al. [34] defined DES as a blend of two or more components with a eutectic temperature that is lower than that of an ideal liquid mixture, with substantial negative deviations from ideality ($\Delta T_2 > 0$). ΔT_2 indicates the depression in temperature, which is the difference between the ideal and real eutectic point. Furthermore, these authors indicated that it is critical that, irrespective of the composition of the mixture, the temperature depression contributes to the liquid mixture at the operating temperature.

Although DESs and traditional ILs have different chemical properties, they have similar physical properties, especially their capacity to be tailored to a specific form of chemistry as tunable solvents. They also possess low vapor pressure, a relatively broad liquid-range, and non-flammability [35]. DESs have many benefits over conventional ILs, such as easy preparation and a convenient supply of comparatively cheap materials (the components themselves are toxicologically well characterized, so they can be conveniently transported for manufacturing on a broad scale); they are, however, less chemically inert in general. The preparation of DESs requires the simple mixing of two or more compounds, usually with moderate heating. With respect to traditional ILs (e.g., imidazolium-based liquids), this yields a relatively low preparation cost and enables large-scale applications. The toxicity of ammonium-based DESs toward bacterial and eukaryotic cells was first investigated by Hayyan et al. [36] and no inhibition of bacterial growth was observed. However, DESs based on phosphonium salts were found to be cytotoxic under the same conditions [37]. Mao et al. [38] found that the toxicity of ChCl-based DESs toward *Arthrobacter simplex* was lower than that of the individual components. The toxicity and biodegradability of DESs toward various organisms (such as, bacterium, *Escherichia coli*) was assessed by Wen et al. [39]. The investigated DESs were toxic to bacteria at concentrations above 75 μM and inhibited bacterial growth by the DESs was much more than that of their individual components. Radosevic et al. [40] investigated the toxicity of three ammonium-based DESs, utilizing fish and human cell lines to measure the in vitro toxicity. All examined DESs were rated as readily biodegradable based on their high degree of mineralization. Many researchers have indicated that DESs has minimal or negligible volatility relative to traditional organic solvents. However, recently, Chen et al. [41] reported the volatilization of ChCl:*N*-methylacetamide (1:6) DES even at room temperature and pressure. Another study conducted by the same group [42] found that the polyethylene glycol (PEG)-based DESs showed volatilization under the same conditions. It is obvious that a better understanding of DESs volatility and toxicity needs more research before these solvents can really be claimed to be less-volatile, biodegradable and non-toxic. A few merits and disadvantages of DESs are presented in Figure 2.

DESs play a significant role in the solubility of gases and liquid-liquid extraction (LLE). Our group [43] compared the performance of classical amine solvents (widely used in the industry for this purpose) and the amine-based DESs for CO₂ capture. The results showed that only 10% of the amine reacted with the CO₂ while for the aqueous solution of MEA, all of the amine reacted with the CO₂. Hence, if only 10% of the amine in the DES reacts with CO₂, this means that the energy needed for desorption is much less than that in amine aqueous solution. In another application related to the use of DESs for separating aromatics from aliphatics, it was noticed that when sulfolane-based DES was used as liquid-liquid extractant, no DES was found in the raffinate layer [44]. While when pure sulfolane was used, its concentration in that layer reached 20 wt%; causing solvent loss and requiring additional purification steps. The same behavior could be predicted for desulfurization and denitrification exposed in this review.

In 2015, García et al. [45] presented a review on the applications of DESs for gas solubility, with special attention to CO₂ capture. Some other reviews involving the capture of CO₂ via DESs have also been published [46–48]. In this work, we present a critical review for the use of different types of DESs in capturing CO₂. Because some reviews about this topic have already been published, we limit the review to the articles published starting from 2015; however, we give more attention to articles published recently. Chen et al. [49] provided a review on the capture of toxic gases by DESs. However, the review about the desulfurization and denitrification of fuels using DESs was not presented. In this study, the use of DESs in the absorption of other hazardous gases, e.g., SO_x, NO_x, NH₃, etc. will be discussed in detail. Furthermore, we will also present in dept review about the desulfurization/denitrification of fuels via DESs. Finally, challenges, opportunities, and perspective of the commercial use of DESs will be discussed.

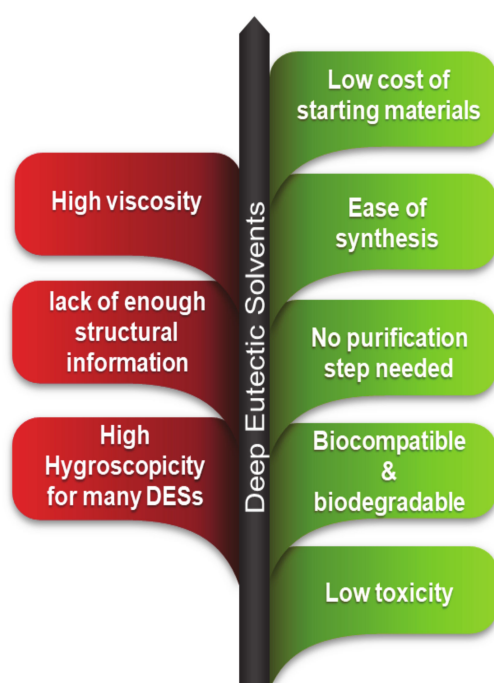


Figure 2. Merits and limitations of DESs as potential solvents [22,48,50].

The main topics of this study are as follows:

- CO₂ capture
- Capture of acidic gases
- Selectivity of DESs in capturing gases
- Desulfurization and denitrification of fuels

2. CO₂ Capture

Chemical absorption, especially amine-based processes, is one of the preferred options for capturing CO₂. However, this process involves some major drawbacks, including the high cost of this technology associated with extensive energy penalties, solvent degradation, and high corrosion [51,52]. The cost of CO₂ separation using amine-based technology is in the range of US \$50 to US \$100 per ton of carbon, which is very high for most of the applications [53]. DESs have become desirable solvents for various gas technology applications due to their beneficial characteristics, such as biodegradability, good thermal and chemical stability, non-flammability, high solvation capability, low-cost, and ease of preparation. This article provides a comprehensive review of the potential applications of DESs for CO₂ capture based on recent studies. Various studies concerning the capture of CO₂ via DESs have already been published; therefore, in this article, we have considered

studies published since 2015. Choline chloride (ChCl)/urea (1:2) is one of the most widely investigated DES for CO₂ capture. The solubility of CO₂ was first measured in ChCl/urea (1:2) DES at 313.15, 323.15, and 333.15 K and at pressures up to 13 MPa [54]. Many factors influence the solubility of CO₂ in DESs, including pressure, temperature, the type of hydrogen bond acceptor (HBA) or HBD, the HBA:HBD molar ratio, viscosity, and the water content of DESs. Table 1 displays the solubility data of CO₂ in various DESs at different temperatures and pressures. We have only included DES systems with CO₂ solubility higher than 0.1 mol CO₂ kg⁻¹ solvent.

Table 1. Solubility (m_{CO_2}) of CO₂ in DESs at different temperatures and pressure.

DES	Molar Ratio	<i>T</i> , K	<i>P</i> , MPa	m_{CO_2} , mol·kg ⁻¹	Refs.
[bmim][MeSO ₃] ¹ /urea	1:1	303.15	0.423	0.245	[55]
ACC ² /1,2,4-triazole	1:1	303.15	0.497	0.186	[56]
ACC/guaiacol	1:3	303.15	0.432	0.127	[57]
	1:4	303.15	0.432	0.133	
	1:5	303.15	0.428	0.140	
ACC/imidazole	2:3	303.15	0.487	0.194	[56]
	1:2	303.15	0.526	0.239	
	1:3	303.15	0.479	0.249	
ACC/LV ³	1:3	303.15	0.543	0.301	[58]
Alanine/lactic acid	1:1	308.15	0.494	0.279	[59]
Alanine/ malic acid	1:1	308.15	0.493	0.346	
ATPPB ⁴ /diethylene glycol	1:4	303.15	0.739	0.174	[60]
	1:10	303.15	0.734	0.145	
	1:16	303.15	0.742	0.122	
ATPPB/triethylene glycol	1:4	303.15	0.718	0.193	[60]
	1:10	303.15	0.744	0.154	
	1:16	303.15	0.744	0.131	
Betaine/lactic acid	1:1	308.15	0.493	0.623	[59]
Betaine/malic acid	1:1	318.15	0.493	0.287	
BHDE ⁵ /acetic acid	1:2	298.15	0.533	0.199	[61]
BHDE/lactic acid	1:2	298.15	0.866	0.122	
BTEA ⁶ /acetic acid	1:2	298.15	0.551	0.265	
BTMA ⁷ /acetic acid	1:2	298.15	0.530	0.271	
ChCl/MEA	1:7	298.15	0.651	2.700	
ChCl/guaiacol	1:3	303.15	0.434	0.116	[57]
	1:4	303.15	0.437	0.121	
	1:5	303.15	0.432	0.129	
ChCl/gly/acetic acid	1:1:1	298.15	0.542	0.112	[61]
DEH ⁸ /guaiacol	1:3	303.15	0.428	0.153	[57]
	1:4	303.15	0.425	0.158	
	1:5	303.15	0.424	0.163	
GUA ⁹ /MEA	1:2	298.15	0.563	0.827	[61]

Table 1. Cont.

DES	Molar Ratio	T, K	P, MPa	m_{CO_2} , mol·kg ⁻¹	Refs.
MTOAB ¹⁰ /decanoic acid	1:2	298.15	0.490	0.285	[62]
MTOAC ¹¹ /decanoic acid	1:2	298.15	0.490	0.297	
MTPPB ¹² /1,2-PD ¹³	1:4	298.15	0.861	0.228	[61]
MTPPB/acetic acid	1:4	298.15	0.652	0.390	
MTPPB/ethylene glycol	1:3	298.15	0.710	0.137	
MTPPB/gly	1:4	298.15	0.875	0.111	
MTPPB/LV	1:3	298.15	0.994	0.161	
MTPPB/LV/ acetic acid	1:3:0.03	298.15	0.516	0.327	
TBAB ¹⁴ /acetic acid	1:2	298.15	0.715	0.380	[61]
TBAB/MEA	1:6	298.15	0.654	1.036	
	1:7	298.15	0.637	1.208	
TBAB/LV	1:3	303.15	0.568	0.269	[58]
TBAB/octanoic acid	1:4	298.15	0.100	0.491	[63]
TBAB/PEG-8	1:4	298.15	0.100	0.286	
TBAC ¹⁵ /acetic acid	1:2	298.15	0.631	0.393	[61]
TBAC/decanoic acid	1:2	298.15	0.490	0.337	[62]
TBAC/LV	1:3	303.15	0.559	0.303	[58]
TEAB ¹⁶ /LV	1:3	303.15	0.564	0.240	
TEAC ¹⁷ /acetic acid	1:2	298.15	0.530	0.284	[61]
	1:3	298.15	0.654	0.315	
TEAC/LV	1:3	303.15	0.562	0.274	
TEAC/octanoic acid	1:3	298.15	0.624	0.342	[61]
TEMA ¹⁸ /acetic acid	1:2	298.15	0.413	0.192	
TEMA/ethylene glycol	1:2	298.15	0.314	0.199	
TEMA/glycerol	1:2	298.15	0.833	0.126	
TEMA/lactic acid	1:2	298.15	0.418	0.109	
TEMA/LV	1:2	298.15	0.409	0.163	
TMAC ¹⁹ /acetic acid	1:4	298.15	0.519	0.296	
TPAC ²⁰ /acetic acid	1:6	298.15	0.554	0.481	
TPAC/MEA	1:4	298.15	0.481	0.338	
	1:7	298.15	0.645	2.051	
TOAB ²¹ /decanoic acid	1:2	298.15	0.490	0.288	[62]
TOAC ²² /decanoic acid	1:1.5	298.15	0.490	0.305	
	1:2	298.15	0.490	0.307	

¹ 1-butyl-3-methyl imidazolium methanesulfonate, ² acetyl choline chloride, ³ levulinic acid, ⁴ allyltriphenylphosphonium bromide, ⁵ N-Benzyl-2-hydroxy-N,N-dimethyl ethanaminium chloride, ⁶ benzyltriethylammonium chloride, ⁷ benzyltrimethylammonium chloride, ⁸ diethylamine hydrochloride, ⁹ guanidinium hydrochloride, ¹⁰ methyltrioctylammonium bromide, ¹¹ methyltrioctylammonium chloride, ¹² methyltriphenyl phosphonium bromide, ¹³ 1,2 propanediol, ¹⁴ tetrabutylammonium bromide, ¹⁵ tetrabutylammonium chloride, ¹⁶ tetraethylammonium bromide, ¹⁷ tetraethylammonium chloride, ¹⁸ triethylmethylammonium chloride, ¹⁹ tetramethylammonium chloride, ²⁰ tetrapropylammonium chloride, ²¹ tetraoctylammonium bromide, ²² tetraoctylammonium chloride.

The unit for the comparison of CO₂ capture is mol·kg⁻¹, except as otherwise mentioned. Deng et al. [58] examined the effect of the HBA of DESs on CO₂ solubility in five LV-based DESs as illustrated in Figure 3a. All DESs were prepared at 1:3 HBA to HBD molar ratio. At fixed temperature (i.e., 303.15 K) and pressure (~0.55 MPa), ACC/LV and TBAC/LV DESs demonstrated the highest CO₂ absorption capacity (around 0.3), while TEAB/LV had the lowest value (0.24). Sarmad et al. [61] also investigated CO₂ capture by various DESs with the HBD as acetic acid (AC). The effect of HBA in the DESs for CO₂ capture was ordered as follows: BTMA (1.45) > TBAC (1.41) > TEAC (1.18) ≈ TEMA (1.18) > TBAB (1.13) > BTEA (0.97) > BHDE (0.84) at a 1:2 molar ratio (HBA:HBD), 298.15 K, and pressure around 2 MPa, as shown in Figure 3b. The authors also examined the effect of the HBD; for example, TEMA-based DESs were prepared by mixing TEMA as the HBA with five different HBDs including AC, ethylene glycol (EG), glycerol (gly), LV and lactic acid (LA) at a 1:2 molar ratio (Figure 3c). The TEMA-based systems followed the order: TEMA/AC (0.61) > TEMA/EG (0.57) > TEMA/LV (0.44) > TEMA/LA (0.37) > TEMA/gly (0.26) at 298.15 K and pressure around 1 MPa. These variations were due to the interactions between CO₂ and functional groups in the HBD. The intermolecular hydrogen bonds are stronger in LA than in AC or LV because of the proximity of the hydroxyl group to the carboxylic group. Hence, it is not easy to break intermolecular hydrogen bonds for contact with CO₂. Furthermore, acetic acid has the weakest intermolecular hydrogen interactions; therefore, acetic acid molecules can readily interact with CO₂, yielding higher CO₂ solubility compared to other DESs. For acetic acid-based DESs, the solubility of CO₂ increases with increasing alkyl chain length of the HBA. For instance, when the alkyl chain length increased from ethyl to butyl (i.e., from tetraethylammonium to tetrabutylammonium), the solubility of CO₂ increased from 1.177 to 1.411 mol·kg⁻¹. Similar behavior was reported by Zubeir et al. [62]; i.e., the solubility of CO₂ increased by increasing the alkyl chain length from methyltrioctyl- to tetraoctylammonium. Moreover, an increase in carbon atoms in the HBD alkyl chain increases CO₂ solubility. This can be attributed to the increase in free volume with increasing alkyl chain length, resulting in higher CO₂ solubility [64]. Li et al. [65] synthesized a series of DESs by mixing different ammonium salts such as HBA and MEA, DEA, MDEA, and TEA as HBDs for CO₂ absorption. The solubility of CO₂ followed the following trend: ChCl ≈ TMAC > TEAC > TEAB > TBAC > TBAB, while for HBD, the order is MEA > DEA > MDEA > TEA. MDEA and TEA showed low CO₂ absorption because of the absence of hydrogen on the nitrogen atoms. The solubility of CO₂ using ChCl and TMAC was almost the same because both salts have similar chemical structures. In Figure 3d, the effect of HBD of ACC-based DESs was investigated at 303.15 K. ACC-based DESs were prepared by mixing with LV, guaiacol (GC), and imidazole (imi) at a 1:3 molar ratio. The order for CO₂ solubility was ACC/LV (0.3) > ACC/imi (0.29) > ACC/GC (0.18).

The nature/type of salt of DESs also plays a crucial role in CO₂ capture. Deng et al. [58] used five ammonium salts (ACC, TEAB, TEAC, TBAB, and TBAC) to prepare DESs for CO₂ capture. For ammonium salts, DESs with larger cations showed higher CO₂ solubility, and the cations of the salts dominated the absorption capacity for CO₂ capture. The performance of various ammonium- and phosphonium-based DESs for CO₂ capture is compared in Figure 4 [43,61]. Both types of DESs with MEA as the HBD resulted in higher CO₂ solubility than the DEA- and TEA-based DESs. The solubility of CO₂ increased by increasing the HBA:HBD molar ratio for ChCl/EA DESs; however, the opposite was true for MTPPB:MEA DES [66].

In general, the solubility of CO₂ in DESs increases with decreasing temperature and increasing pressure. Sarmad et al. [61] investigated the effect of pressure on the CO₂ capture via various DESs, as shown in Figure 5. As expected, the solubility of CO₂ in the DESs increased with increasing pressure and decreasing temperature for the systems examined. The decrease in solubility with increasing temperature can be understood using the concept of the kinetic energy of the gas molecules: as it increases with increasing temperature,

causing breakage of intermolecular bonds between the gas molecules that are formed within the solute, and these have a higher tendency to escape from the solution.

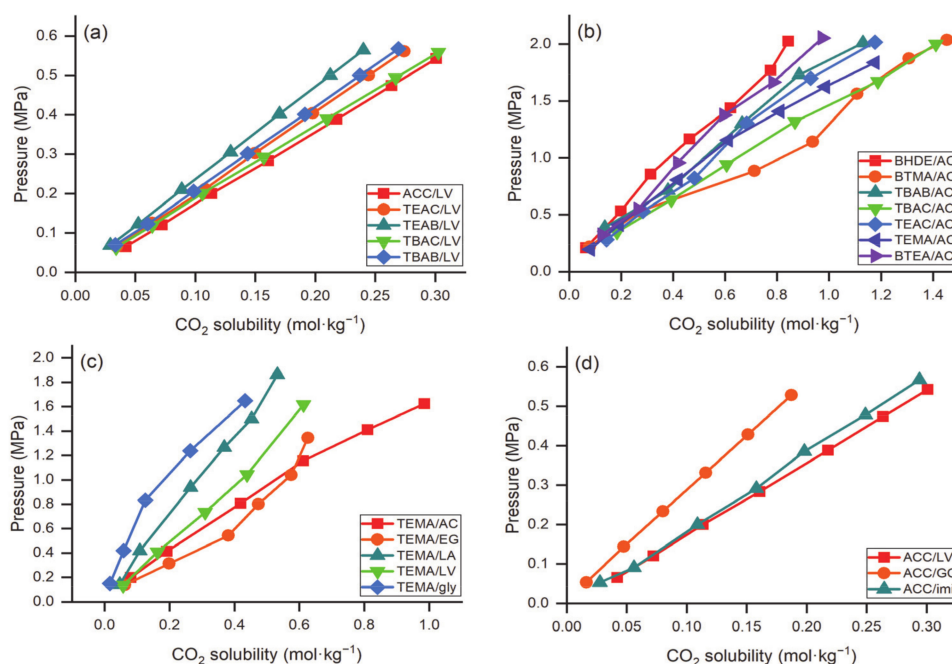


Figure 3. Effect of (a) HBA of LV-based DESs on CO₂ solubility at 303.15 K, (b) HBA of AC-based DESs on CO₂ solubility at 298.15 K, (c) HBD of TEMA-based DESs on CO₂ solubility at 298.15 K, and (d) HBD of ACC-based DESs on CO₂ solubility at 303.15 K, data are extracted from [56,57,61].

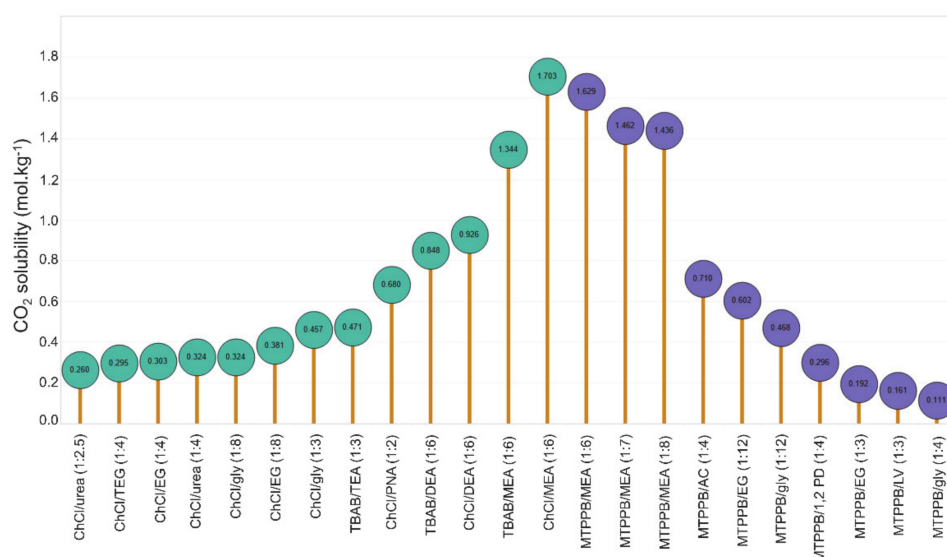


Figure 4. CO₂ solubility in ammonium and phosphonium-based DESs at around 1 MPa, and 298.15 K. Data are taken from [43,61].

Usually, the solubility of CO₂ in the DESs follows Henry's Law (Equation (1)), i.e., the solubility of CO₂ is proportional to its partial pressure. Deng et al. [58] also investigated the effect of pressure on CO₂ solubility in five LV-based DESs. They found that the solubility of CO₂ in DESs is proportional to the gas phase's equilibrium pressure, indicating that the CO₂ absorption via DES is a physical phenomenon. Figure 5a depicts the CO₂ solubility as a function of pressure in various DESs. It is evident from the figure that the solubility

increases with increasing pressure for all the DESs. Figure 5b shows the effect of pressure on TEAC/LV (1:3) at different temperatures. Solubility trends have shown that the CO₂ absorption capacity increases with decreasing temperature and increasing pressure.

The degree of gas solubility in a solvent is often assessed using Henry's law constant (k_H) [67]:

$$k_H = \lim_{x_i \rightarrow 0} \left(\frac{f_i}{x_i} \right) \quad (1)$$

where x_i is the mole fraction of gas in the solution, and f_i is the gas fugacity in vapor phase.

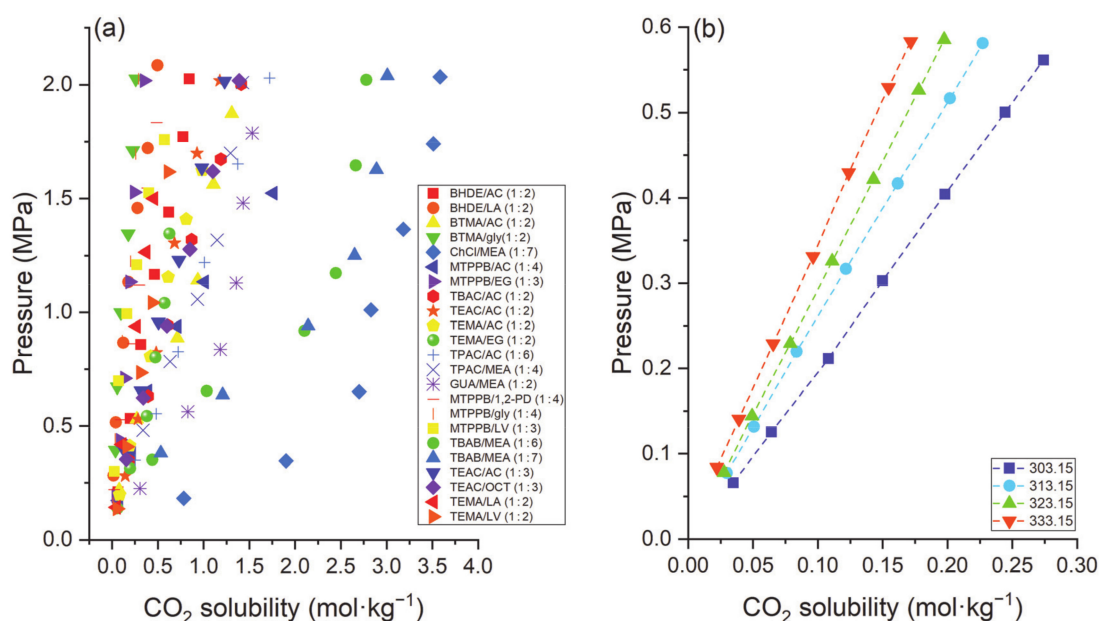


Figure 5. Effect of pressure on (a) various DESs at 298.15 K, and (b) TEAC/LV (1:3) DES at different temperatures. Data are extracted from [58,61].

Liu et al. [57] reported that the solubility of CO₂ increases with an increase in the mole fraction of ChCl/GC, DEH/GC, and ACC/GC from 1:3 to 1:5 at a fixed pressure and temperature, indicating that GC plays a major role in the solubility of CO₂ in DESs. For example, the solubility of CO₂ using ChCl/GC increased from 0.171 to 0.188 when molar ratio was changed from 1:3 to 1:5. Furthermore, the effect of the molar ratio of DESs on Henry's law constant of CO₂ absorption was also obvious. Among GC-based DESs, DEH/GC (1:5) showed the lowest Henry's law constant, i.e., higher CO₂ solubility at a fixed temperature and pressure. The effect of the molar ratio of different amine-based DESs on the solubility of CO₂ was also investigated [66]. The solubility of CO₂ increased with a decrease in the molar ratio of ChCl/MEA and ChCl/DEA DESs from 1:6 to 1:10, indicating that addition of MEA or DEA can increase both the chemical and physical absorption of CO₂. However, Ghaedi et al. [60] found that by increasing the molar ratio of phosphonium-based DESs including ATPPB/diethylene glycol (DEG), and ATPPB/triethylene glycol (TEG) from 1:4 to 1:16, the solubility of CO₂ decreased as shown in Figure 6. This result demonstrated that ATPPB plays an important role in CO₂ capture. At the same time, glycols play a minor role. Ren and co-workers [68] explored the effect of L-arginine/gly molar ratios (1:5, 1:6, and 1:7) on the solubility of CO₂.

Many DESs are highly hygroscopic and tend to absorb water easily [69]. Ren et al. [68] exploited the hydrophilic nature of DESs for CO₂ capture. DESs with varying water content have been tested for CO₂ capture to explore the effect of water content on CO₂ solubility. They found that the efficiency of CO₂ capture could be increased by adding a small amount of water to the DES. Ma et al. [70] investigated the effect of water on CO₂ solubility using glycerol-based DESs. Most of the glycerol-based DESs have high viscosity; however, for

some DESs, viscosity changes drastically when a small amount of water is added [71]. For instance, the viscosity of BTMA/gly (1:2) DES was reduced from 716 to 20 mPa·s after adding a small quantity of water (0.11 mole fraction).

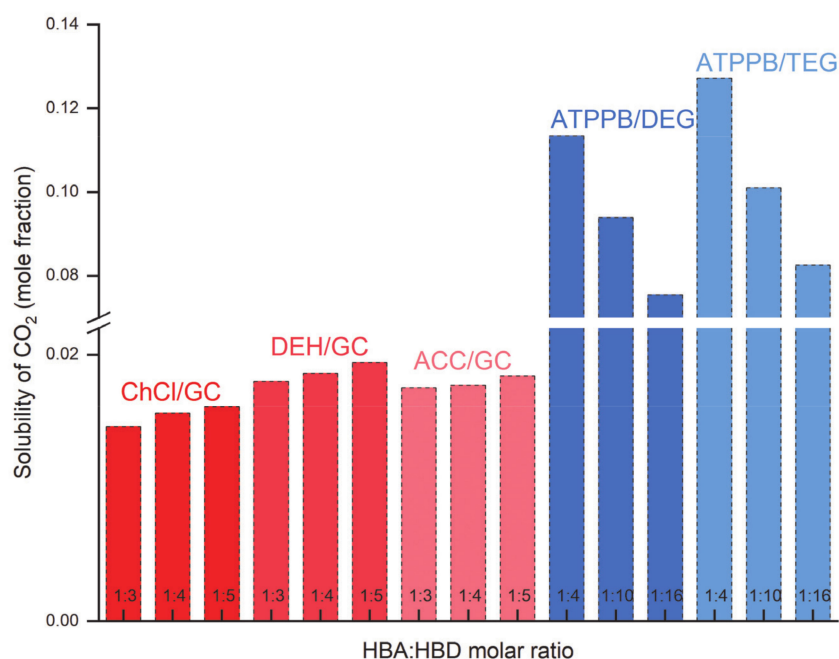


Figure 6. Effect of the molar ratio of DESs on the solubility of CO₂ at 303.15 K and under 0.5 MPa. Data are extracted from [57,60].

Furthermore, CO₂ absorption increased by 25% using BTMA/gly (1:2) with 0.11 mole fraction of water. However, the solubility of CO₂ was reduced by further increasing the water content owing to the low solubility of CO₂ in water. Trivedi et al. [72] examined the absorption of CO₂ in the presence of varying water content (5–20 wt%) with monoethanolamine hydrochloride /ethylenediamine (1:3) DES. With an increase in water content, the initial uptake kinetics were improved, i.e., when the water quantity increased from 0 to 20 wt%, CO₂ uptake increased from 25.2 to 28.1 wt%.

3. Capture of Acidic Gases

Nitric oxide (NO), nitrogen oxide (NO₂), ammonia (NH₃), sulfur dioxide (SO₂), and hydrogen sulfide (H₂S) are considered toxic industrial gases [49]. The burning of coal mainly produces NO₂ and NO. Large amounts of these oxides (NO and NO₂) can cause acid rain, acid mist, destruction of ozone, and harm to human health. NH₃ is often generated from waste gas during the synthesis of ammonia, which causes air pollution and rhinitis/pharyngitis and facilitates the formation of particulate matter. During the combustion of fossil fuels from industrial waste gas or volcanic eruptions, toxic SO₂ is produced. Air pollution, human cancer, and acid rain result from the release of large quantities of SO₂ [73]. H₂S is another acidic gas produced from natural gas treatment, decomposition of bacteria, and industrial refineries. H₂S has high toxicity and corrosiveness. Due to the high risk of these acidic gases (i.e., SO₂, NH₃, H₂S, NO₂, and NO), high-performance, low-cost, and highly sustainable processes are required to capture them. It is clear that toxic gas capture can enhance air quality, reduce air pollution, and preserve the ozone layer. In addition, the captured gas can be utilized in other processes. Hence, it is imperative to have green routes to capture these toxic gases with better efficiency and selectivity.

The solubility of these gases in the solvent is an essential factor for the absorption of these gases. The solubility data for oxide-based acidic gases in various DESs and ILs are shown in Table 2.

Table 2. Solubility of SO₂ (m_{SO_2} , g SO₂/g DES), NO (m_{NO} , mol NO/mol DES), and NO₂ (m_{NO_2} , g NO₂/g DES) in DESs and ILs at 0.1 MPa.

DES	Molar Ratio	m_{SO_2} , (T, K)	m_{NO} , (T, K)	m_{NO_2} , (T, K)	Refs.
Deep eutectic solvents					
ACC/1,2,4-triazole	1:1	0.227 (303.2) ¹			[74]
ACC/imidazole	1:1.5	0.356 (303.2) ¹			
ACC/LV	1:3	0.567 (293)			[75]
ACC/imidazole	1:2	0.989 (303.2)			[74]
	1:3	0.383 (303.2) ¹			
Betaine/EG	1:3	0.366 (313.2)			[76]
BMIMB ² /acetamide	1:1	1.00 (303.2)			[77]
BMIMB/DMU ³	1:1	0.920 (293.2)			[78]
BMIMC/ethyleneurea	1:1	1.07 (293.2)			
BMIMC/acetamide	1:1	1.17 (303.2)			[77]
BMIMC ⁴ /DMU	1:2	0.950 (293.2)			
	1:1	1.04 (293.2)			[78]
	2:1	1.14 (293.2)			
BMIMC/Mim ⁵	1:1	1.31 (293.2)			
	1:2	1.42 (293.2)			
BMIMC/imidazole	2:1	1.32 (293.2)			[79]
	1:1	1.29 (293.2)			
	1:2	1.24 (293.2)			
ChCl/gly	1:1	0.678 (293.2)			[80]
	1:2	0.482 (293.2)		0.356 (298.2)	[80,81]
	1:3	0.380 (293.2)			[80]
	1:4	0.320 (293.2)		0.371 (298.2)	[80,81]
ChCl/LV	1:3	0.557 (293.2)			[75]
ChCl/GC	1:3	0.528 (293.2)			
	1:4	0.501 (293.2)			
	1:5	0.479 (293.2)			
ChCl/cardanol	1:3	0.196 (293.2)			[82]
	1:4	0.170 (293.2)			
	1:5	0.149 (293.2)			
ChCl/EG	1:2	0.700 (293.2)		0.396 (298.2)	[81,83]
	1:4			0.551 (298.2)	[81]
ChCl/malonic acid	1:1	0.490 (293.2)			
ChCl/urea	1:2	0.350 (293.2)			[83]
ChCl/thiourea	1:1	0.880 (293.2)			
ChCl/tetrazolium	1:1	0.860 (343.2)			
ChCl/triazole	1:1	0.670 (343.2)			[84]
ChCl/imid	1:1	0.470 (343.2)			

Table 2. Cont.

DES	Molar Ratio	m_{SO_2} , (T, K)	m_{NO} , (T, K)	m_{NO_2} , (T, K)	Refs.
Caprolactam/imidazole	1:1	1.66 (303.2)			[85]
Caprolactam/acetamide	1:1	0.988 (303.2)			
Carnitine/EG	1:3	0.365 (313.2)			[76]
EMIMB/ethyleneurea	1:1	0.910 (293.2)			[78]
EMIMC ⁶ /DMU	1:1	1.14 (293.2)			
EMIMC/EG	2:1	1.15 (293.2)			[86]
	1:1	1.03 (293.2)			
	1:2	0.820 (293.2)			
EMIMC/TEG	1:1	0.910 (293.2)			[87]
	2:1	1.06 (293.2)			
	4:1	1.20 (293.2)			
	6:1	1.25 (293.2)			
EMIMC/succinonitrile	1:1	1.13 (293.2)			[88]
	1:2	0.960 (293.2)			
	1:4	0.790 (293.2)			
EMIMC/FMP ⁷	1:1	0.220 (293.2)			[89]
	1:2	0.162 (303.2)			
	2:1	0.245 (303.2)			
EMIMC/acetamide	1:1	1.25 (303.2)			[77]
	1:2	1.13 (303.2)			
	2:1	1.39 (303.2)			
EMIMC/imidazole	2:1	1.40 (293.2)			[90]
EMIMC/1,2,4-triazole	2:1	1.28 (293.2)			
EMIMC/1,2,3-triazole	2:1	1.18 (293.2)			
EMIMC/tetrazole	2:1	1.13 (293.2)			
EMIMC/EPB ⁸	1:1	1.29 (293.2)			[91]
	2:1	1.34 (293.2)			
	3:1	1.39 (293.2)			
EMIMC/ethyleneurea	1:1	1.14 (293.2)			[78]
HMIMC ⁹ /acetamide	1:1	1.02 (303.2)			[77]
Imidazole/gly	1:2	0.163 (313.2)	0.034 (313.2)		[92]
KSCN ¹⁰ /acetamide	1:3	1.43 (293.2)			[93]
KSCN/caprolactam	1:3	1.54 (293.2)			
NH ₄ SCN ¹¹ /acetamide	1:3	1.37 (293.2)			
NH ₄ SCN/caprolactam	1:3	1.47 (293.2)			[94]
PPZB ¹² /gly	1:4	0.420 (293.2)			
	1:5	0.380 (293.2)			
	1:6	0.350 (293.2)			

Table 2. Cont.

DES	Molar Ratio	m_{SO_2} , (T, K)	m_{NO} , (T, K)	m_{NO_2} , (T, K)	Refs.
TBAB/caprolactam	1:1	0.747 (293.2)			[95]
	1:2	0.764 (293.2)			
	1:3	0.719 (293.2)			
	1:4	0.696 (293.2)			
TBAB/LV	1:3	0.547 (293.2)			[75]
TBAB/Tetz ¹³	1:1		0.320 (303.2)		[84]
TBAB/DMTU ¹⁴	1:1		1.00 (303.2)		[96]
TBAB/imidazole	1:2	0.910 (293.2)			[79]
TBAB/caprolactam	1:2		0.090 (343.2)		[97]
TBAC/Mim	1:2	1.04 (293.2)			
TBAC/imidazole	1:2	0.960 (293.2)			
TBAC/benzimidazole	1:2	0.820 (293.2)			[79]
TBAC/pyrazole	1:2	0.710 (293.2)			
TBAC/tetrazole	1:2	0.460 (293.2)			
TBAC/ethyleneurea	1:1	0.810 (293.2)			[78]
TBAC/LV	1:3	0.541 (293.2)			[75]
TBAC/Tetz	1:1		1.46 (303.2)		[84]
TBAC/DMU	1:1	0.830 (293.2)			[78]
TBAC/DMTU	1:1	0.830 (293.2)	2.05 (303.2)		[96]
TBAC/caprolactam	1:2		0.130 (343.2)		[97]
TBAF ¹⁵ /caprolactam	1:2		0.160 (338.2)		
TBPB ¹⁶ /Tetz	1:1		0.480 (303.2)		[84]
TBPB/DMTU	1:1		1.13 (303.2)		
TBPB/DMU	1:1		0.660 (293.2)		[96]
	1:2		0.920 (293.2)		
	1:3		1.17 (293.2)		
TBPC ¹⁷ /Mim	1:2	1.04 (293.2)			[79]
TBPC/DMU	1:1	0.830 (293.2)			[78]
TBPC/ethyleneurea	1:1	0.810 (293.2)			
TBPC/Tetz	1:1		2.10 (303.2)		
TBPC/Imid	1:1		0.160 (303.2)		[84]
TBPC/triazole	1:1		0.710 (303.2)		
TBPC/DMTU	1:1		2.13 (303.2)		[96]
	1:2		3.18 (303.2)		
	1:3		4.25 (303.2)		
TEAB/LV	1:3	0.622 (293.2)			
TEAC/LV	1:3	0.625 (293.2)			[84]
Ionic Liquids					
[Emim][SCN]		1.13 (293.2)			[98]
[NEt ₂ C ₂ Py][SCN]		1.06 (293.2)			[99]

Table 2. Cont.

DES	Molar Ratio	m_{SO_2} , (T, K)	m_{NO} , (T, K)	m_{NO_2} , (T, K)	Refs.
[E ₃ Py][Cl]		1.05 (293.2)			[100]
[E ₃ Eim ₂][Cl] ₂		1.03 (293.2)			[101]
[Et ₂ NEMim][Tetz]		1.10 (293.2)			[102]
[C ₄ Py][SCN]		0.841 (293.2)			[103]

¹ at 0.01 MPa, ² 1-butyl-3-methylimidazolium bromide, ³ 1,3-dimethylurea, ⁴ 1-butyl-3-methylimidazolium chloride, ⁵ 4-methylimidazole, ⁶ 1-ethyl-3-methylimidazolium chloride, ⁷ *N*-formylmorpholine, ⁸ *N*-ethylpyridinium bromide, ⁹ 1-Hexyl-3-methyl-imidazolium chloride, ¹⁰ potassium thiocyanate, ¹¹ ammonium thiocyanate, ¹² 1-hydroxyethyl-1,4-dimethyl-piperazinium bromide, ¹³ tetrazolium, ¹⁴ 1,3-dimethylthiourea, ¹⁵ tetrabutyl ammonium fluoride, ¹⁶ tetrabutyl phosphonium bromide, ¹⁷ tetrabutyl phosphonium chloride.

3.1. Oxide-Based Acid Gases

3.1.1. SO₂ Capture

Yang et al. [80] investigated the solubility of SO₂ in ChCl/gly DES with different molar ratios. Figure 7 shows the effect of ChCl/gly DES molar ratio on the solubility of SO₂ at different temperatures. The highest SO₂ solubility (0.678 g SO₂/g DES) using ChCl/gly was achieved at 1:1 molar ratio, 0.1 MPa, and 293.15 K. An increase in the HBD molar ratio from 1:1 to 1:4 at fixed pressure and temperature reduced the SO₂ absorption capacity. For instance, at 293.2 K and 0.1 MPa, the solubility of SO₂ was reduced from 0.678 to 0.320 (g SO₂/g DES). The effect of a mole fraction of ChCl/gly DES on Henry's law constant of SO₂ absorption was also evident. Henry's law constant increased with decreasing concentrations of ChCl in the DES. The same group [104] investigated the solubility of SO₂ in another DES formed by combining EMIMC with EG under different operating conditions. The absorption capacity of SO₂ increased (0.82, 1.03 to 1.15 g SO₂/g DES) with an increase in the ratio of EMIMC in EMIMC:EG DES (from 1:2 to 1:1 and 2:1). The same group prepared EMIMC-based DESs by mixing EMIMC with either TEG or succinonitrile (SNT) to investigate the SO₂ absorption capacity [105]. The SO₂ absorption capacity increased with an increase in the molar ratio of EMIMC in the EMIMC/TEG DES. The highest capacity of 1.25 g SO₂/g DES was achieved in the EMIMC/TEG at a 6:1 molar ratio.

It is interesting to note that in some cases, increasing the molar ratio of HBD increased the SO₂ solubility. In contrast, in other cases, the solubility was increased by increasing the molar ratio of HBA. For example, the solubility of SO₂ increased when the molar ratio of ChCl or EMIMC in ChCl/phenol, ChCl/gly, EMIMC/EG, EMIMC/TEG and EMIMC/FMP DESs was increased [82,89]. However, SO₂ solubility increased with increasing molar ratio of imidazole in ACC/imidazole DES because imidazole exhibited a strong interaction with SO₂ [74]. A significant change in SO₂ solubility was observed with the change in the molar ratio of ChCl and EMIMC-based DESs; however, that is not true for all DESs. For instance, betaine:EG and caprolactam:EG showed almost no change in SO₂ absorption at different molar ratios (1:3 to 1:5) [49,76]. Similarly, a change in the molar ratio of PPZB/gly DES had almost no effect on the capacity of SO₂ [94].

Yang et al. [106] investigated the effect of HBD of DESs [EMIMC/EG (1:1), EMIMC:TEG (1:1), and EMIMC:SNT (1:1)] on the solubility of SO₂. The effect of HBD was ordered as SNT > EG > TEG for SO₂ capture. The absorption capacity of SO₂ by ChCl-based DESs was ordered as ChCl/thiourea (1:1) > ChCl/EG (1:2) > ChCl/malonic acid (1:1) > ChC/urea (1:2) at 0.1 MPa and 293.2 K [83]. Zhang et al. [92] prepared four DESs based on imidazole and its derivatives to explore their performance with regard to SO₂ capture. Imidazole, 2-methylimidazole, 2-ethylimidazole, and 2-propylimidazole were mixed with glycerol at a 1:2 molar ratio. Among the four DESs, the highest solubility of SO₂ (0.253 g SO₂/g DES at 0.002 MPa and 313.2 K) was achieved using imidazole/gly (1:2) DES [92]. Deng et al. [75] studied the solubility of SO₂ in six DESs composed of quaternary ammonium

salts (ChCl, ACC, TEAC, TEAB, TBAC, and TBAB) as the HBA and LV as the HBD at a 1:3 (HBA:HBD) molar ratio.

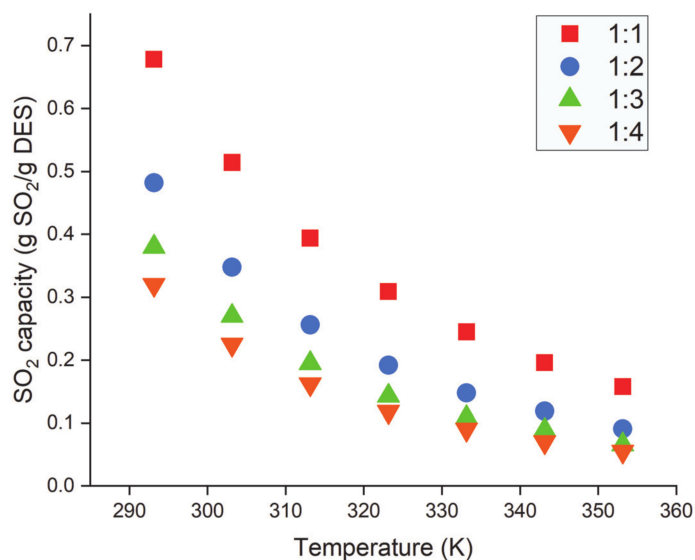


Figure 7. Effect of temperature and molar ratio on SO₂ capture capacity by ChCl/gly. Data are extracted from [80].

The highest solubilities were obtained using TEAC/LV and TEAB/LV DES at all temperatures (293.2–343.2 K), as shown in Figure 8a. Long et al. [90] investigated the performance of four bisazole-based DESs in SO₂ capture. The DESs were obtained by mixing EMIMC with imidazole, 1H-1,2,4-triazole, 1,2,3-1H-triazole, or tetrazole in a 2:1 (HBA:HBD) molar ratio. The effect of HBDs on SO₂ capacity was examined at 293.2 K and 0.1 MPa, as illustrated in Figure 8b. The effect of HBDs on the solubility of SO₂ was evident. TBAC was mixed with imidazole, 4-methylimidazole, pyrazole, tetrazole, and benzimidazole at a 1:2 molar ratio. Equilibrium was reached in 10 min, and the absorption capacities of SO₂ were as follows: 4-methylimidazole > imidazole > benzimidazole > pyrazole > tetrazole. For EMIMC-based DESs, the effect of HBD in DESs on SO₂ capture at all temperatures and 0.1 MPa was as follows: EMIMC/imidazole > EMIMC/1H-1,2,4-triazole > EMIMC/1,2,3-1H-triazole > EMIMC/tetrazole. It is also evident from Figure 8a that temperature plays a significant role in the capture of SO₂ by DESs. SO₂ capture via DESs decreased linearly with increasing temperature. Yang et al. also reported that the absorption capacity of SO₂ using EMIMC/EG, EMIMC/TEG, and EMIMC/SNT decreased with increasing temperature [104–106].

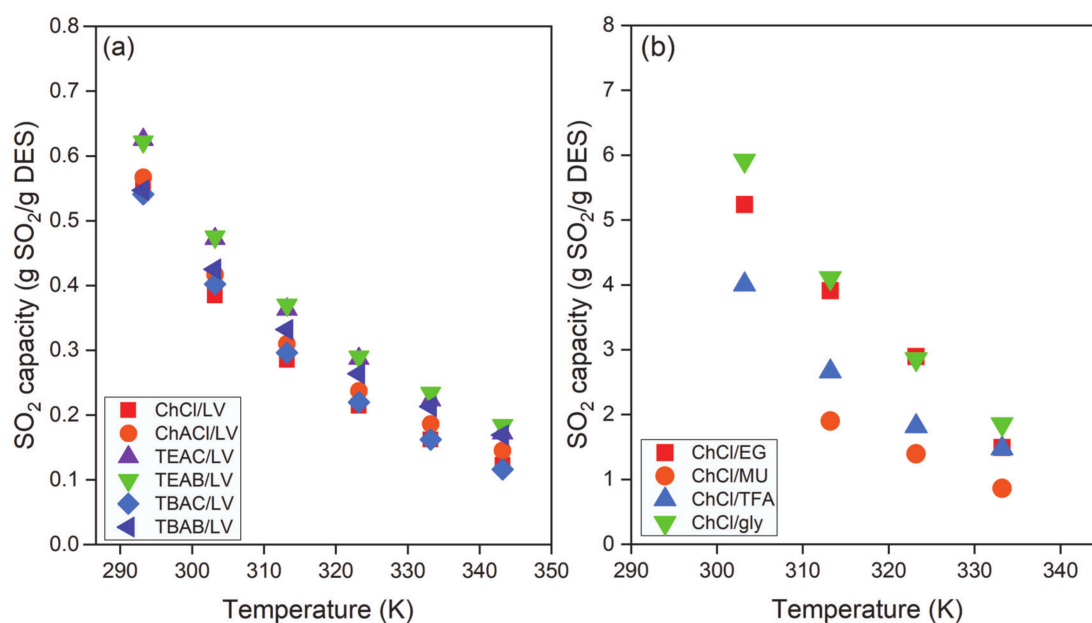


Figure 8. Effect of (a) HBA and (b) HBD on SO_2 capacity at 0.1 MPa as a function of temperature. Data are extracted from [75,79].

3.1.2. NO_x Capture

A limited number of studies have reported on the absorption of NO via DESs. Zhang et al. [92] used imidazole/gly (1:2) to capture NO. They used the same DES to capture SO_2 and found that it had a very low capacity (0.034 mol NO/mol DES) for NO compared to SO_2 (0.643 mol SO_2 /mol DES). Azole-based DESs were found to be efficient at dissolving NO. Zhang et al. [84] used four azole-based low-viscosity DESs to capture NO. TBPC/Tetz (1:1) exhibited the highest NO absorption capacity: 2.10 mol NO/mol DES at 0.1 MPa and 303.2 K. These researchers also studied the effect of temperature on the absorption capacity of NO, as shown in Figure 9a. The absorption capacity of NO decreased linearly with the increase in temperature. The authors found that there were chemical interactions between the hydrogen attached to the ring containing the nitrogen atom of Tetz and NO. The effect of HBA in DESs on the solubility of NO was also examined. The effect of HBA in DESs on NO capture at 0.1 MPa and 303.2 K was as follows: TBPC/Tetz > TBAC/Tetz > TBPB/Tetz > TBAB/Tetz. Moreover, lower NO pressure and higher temperature reduced the absorption capacity of the DESs. Sun et al. [107] explored the application of amine-based functional DESs for the capture of NO. The DESs were prepared by mixing ammonium salts with polyhydric alcohols, and all DESs showed good absorption capacity for NO (10 vol%). Sun et al. [107] also investigated the effect of temperature on the DES absorption capacity of NO. For example, the absorption capacity decreased from 0.33 to 0.18 mol NO/mol DES, with increasing temperature from 303.2 to 323.2 K in tetraethylenepentamine chloride (TEPA)/EG (1:3) DES. This could be attributed to the weak binding forces between NO and DES at higher temperatures. Owing to the increase in temperature, the equilibrium shifted in the opposite direction, causing reduction in the NO absorption capacity.

The effect of the molar ratio of DESs on the absorption capacity of NO was also investigated. For instance, NO absorption capacity increased from 3.10 to 4.52 mol NO/mol DES when the molar ratio of TEPA/EG changed from 1:1 to 1:3.

No change in the molar absorption capacity of NO was observed when the molar ratio further changed from 1:4 to 1:6. However, the mass absorption capacity of NO was reduced with the increase in EG from 1:4 to 1:6, which indicated that the active constituent affecting the NO absorption capacity was TEPA [107]. In another study, Sun et al. [96] reported that the absorption capacity of NO increased for TBPB/DMTU DES as the molar ratio increased from 1:1 to 1:3.

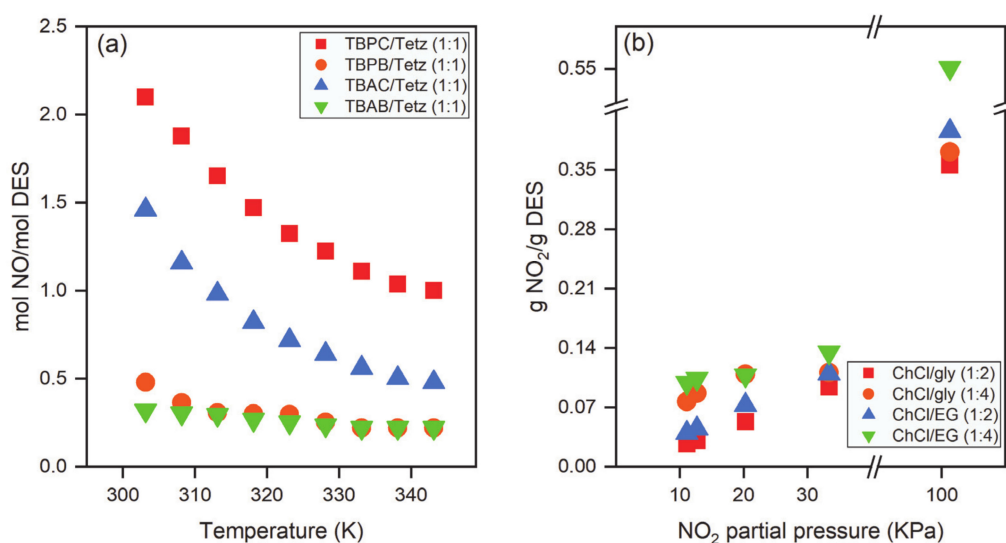


Figure 9. Effect of (a) temperature and HBA on the absorption capacity of NO, (b) partial pressure on NO₂ solubilities in four ChCl-DESs at 298.15 K [81,84].

The effect of water on the absorption capacity of NO was also explored, and no significant change in the NO absorption capacity by TEPA/EG (1:3) DES was observed under different levels of water content [107]. For example, the mass absorption capacities of NO using TEPA/EG (1:3) DES were 0.30 and 0.32 mol NO/mol DES when the water content of the DES was 18.3 and 0.1 wt%, respectively. However, the mass transfer rate was improved with increasing water owing to a reduction in the viscosity of the DES.

Although applications of DESs for the capture of acid gases continue to emerge, DES absorption of NO₂ is still in the embryonic stage. Recently, Chen et al. [81] studied the absorption of NO₂ by ChCl-based DESs and their aqueous mixtures. The effect of the partial pressure of NO₂ on the absorption capacity of DESs was analyzed at 298.15 K, as shown in Figure 9b. With decreasing NO₂ partial pressure, the solubility of NO₂ was reduced. For example, the solubility in ChCl/gly (1:2) was reduced from 0.356 to 0.027 gNO₂/gDESs when the partial pressure was decreased from 101.3 to 0.01 MPa. The effect of the molar ratio of DESs on the absorption capacity was also investigated, and the solubility was increased with increasing molar ratio. The effect of water content on NO₂ absorption capacity was also explored. With the addition of 3–6 wt% water, the solubility of NO₂ in the DESs showed the following trend: ChCl/gly (1:2) > ChCl/EG (1:2) > ChCl/gly (1:4) > ChCl/EG (1:4). With high water content (more than 50 wt% water), NO₂ absorption is unfavorable. At this water concentration, the DES becomes unstable, and a complex hydrogen bond network among the components of the DES and water is formed, as reported previously [81].

Other studies relevant to the absorption of NO₂ in DESs were based on theoretical calculations alone. For instance, the absorption mechanism of NO₂ in ChCl DESs with urea, methyl urea, and thiourea as HBD was investigated using quantum chemical methods [108]. Based on quantum calculations, ChCl/thiourea was found to be more favorable for denitrification. However, experimental data are needed to verify such predictions.

3.2. NH₃ Capture

The excellent benefits of simple synthesis and high tunability have yielded a wide range of prospects for evolving DESs. Various configurations and combinations of HBA and HBD make DESs rich and diverse, affecting the physicochemical properties of these DESs and their ability to absorb NH₃. This section focuses on the solubility of NH₃ by various DESs. As illustrated in Table 3, NH₄SCN, ChCl, and 1-ethyl-3-methylimidazolium ([emim]Cl) are the most widely used HBAs to absorb NH₃. These HBAs are usually mixed

with HBDs such as glycerol, EG, urea, benzoic acid, LV, and phenol to form DESs in a specific molar ratio.

Table 3. The solubility of NH_3 (m_{NH_3} , $\text{mol}\cdot\text{kg}^{-1}$) in DESs at different temperature (K) and pressure (MPa).

DES	Molar Ratio	Temperature	Pressure	m_{NH_3}	Refs.
1,2,4-triazole/gly	1:3	313.15	0.10	6.706	[109]
ChCl/1,4-BD ¹	1:3	313.15	0.13	2.347	[110]
ChCl/2,3-BD ²	1:4	313.15	0.12	2.369	
	1:3	313.15	0.13	2.073	
ChCl/1,3-PD ³	1:4	313.15	0.12	1.903	
	1:3	313.15	0.13	2.513	
ChCl/EG	1:4	313.15	0.12	2.517	[111]
	1:2	333.2	0.10	1.491	
ChCl/gly	1:2	333.2	0.11	1.341	
ChCl/MU ⁴	1:2	333.2	0.09	0.519	
ChCl/xylose	1:1	333.2	0.11	4.187	
	1.5:1	333.2	0.11	3.722	[112]
	2:1	333.2	0.10	2.980	
ChCl/TFA ⁵	1:2	333.2	0.12	1.475	[111]
ChCl/phenol/EG	1:5:4	313.2	0.10	6.988	[113]
	1:7:4	313.2	0.10	7.652	
ChCl/imidazole/EG	3:7:14	313.2	0.10	4.909	[106]
ChCl/triazole/EG	3:7:14	313.2	0.10	6.495	
ChCl/tetrazole/EG	3:7:14	313.2	0.11	9.952	
ChCl/urea	1:1.5	313.2	0.11	1.436	[114]
	1:2	313.2	0.11	1.599	
	1:2.5	313.2	0.10	1.355	
ChCl/PNA ⁶	1:2	313.2	0.10	2.445	[115]
ChCl/LV	1:2	313.2	0.10	4.631	[116]
	1:4	298.2	0.10	9.494	
	1:5	298.2	0.10	9.443	
EaCl/AA ⁷	1:1	313.2	0.10	3.830	[117]
	1:2	313.2	0.10	3.600	
	1:3	323.2	0.10	2.210	
EaCl/phenol	1:2	313.2	0.10	7.023	[118]
	1:3	313.2	0.10	7.433	
	1:5	313.2	0.10	8.106	
	1:7	298.2	0.10	9.801	
EaCl ⁸ /gly	1:2	298.2	0.11	9.631	[116]
EaCl/urea	1:0.5	313.2	0.10	4.396	[119]
	1:1	313.2	0.10	4.573	
	1:2	313.2	0.10	4.179	

Table 3. Cont.

DES	Molar Ratio	Temperature	Pressure	m_{NH_3}	Refs.
GI ⁹ /AA	1:2	303.15	0.10	5.300	
	1:3	303.15	0.10	4.160	[120]
	1:4	303.15	0.10	3.580	
Imidazole/gly	1:3	313.15	0.10	5.812	[109]
KSCN/gly	2:3	313.15	0.10	5.970	[121]
MAA ¹⁰ /tetrazole	2:1	313.2	0.10	8.000	
	2.5:1	313.2	0.10	6.650	
	3:1	313.2	0.10	5.940	[122]
MAA/imidazole	2:1	313.2	0.11	1.770	
MAA/triazole	2:1	313.2	0.10	3.650	
NH ₄ SCN/gly	2:3	313.15	0.10	10.36	
NH ₄ SCN/EG	1:3	313.15	0.10	9.890	
NH ₄ SCN/urea	2:3	313.15	0.10	8.590	[121]
NH ₄ SCN/acetamide	2:3	313.15	0.10	5.390	
NH ₄ SCN/caprolactam	1:3	313.15	0.10	1.730	
Tetrazole/gly	1:3	33.15	0.10	8.929	[109]

¹ 1,4-butanediol, ² 2,3-butanediol, ³ 1,3-propanediol, ⁴ N-Methyl urea, ⁵ trifluoroacetamide, ⁶ phenylacetic acid, ⁷ acetamide, ⁸ ethylamine hydrochloride, ⁹ guanidine isothiocyanate, ¹⁰ methylacetamide.

The effect of the HBA and HBD of DESs is depicted by heat map induction, as shown in Figure 10. For the same molar ratio (1:2), ChCl-based DESs showed the following order for NH₃ solubility: LV > gly > PNA > EG > TFA > urea > MU. During absorption by DESs, white solid particles were formed with the acidic HBDs (LV or PNA), which severely hindered NH₃ interaction with the remaining absorbent and prevented further absorption. The breaking up of the supramolecular structure in the DES resulted in solid formation. This mechanism's adverse consequence is well illustrated by the peculiar relationship between acidity and capacity in these solvents' absorption.

Since carboxylic acids are even more acidic than alcohols and urea, DESs containing carboxylic acids as HBDs were assumed to have a higher NH₃ uptake ability than ChCl/gly, ChCl/EG, and ChCl/urea. However, these predicted outcomes were not achieved [115]. This unexpected acidity–capacity relationship revealed that the well-recognized approach to increase the solubility of simple solutes by raising the acidity or their number of acidic groups of solvents is not generally true in the case of DESs because of the fragile supramolecular structure. In order to prevent this structural breakage, ternary DESs can be prepared by adding neutral donors. However, the opposite behavior was observed when acidic HBAs were used. For instance, Deng et al. [109] compared the performance of three azole-based DESs, and found that NH₃ solubility increased with increasing HBA acidity as follows: tetrazole/gly > 1,2,4-triazole/gly > imidazole/gly. They also investigated the effect of HBD of DES on the solubility of NH₃. Triazole was mixed with six different HBDs (caprolactam, acetamide, glycerol formal, DL-1,2-isopropylidene glycerol, EG, and glycerol). Higher solubility of NH₃ was observed for the DESs containing a hydroxyl group as the HBD.

The addition of a third component to the binary DESs can affect the solubility of NH₃. Zhong et al. [123] prepared a ternary DES by combining ChCl with EG and tetrazole and compared the solubility of NH₃ of ternary DES with ChCl/EG and EG. ChCl/tetrazole/EG (3:7:14) showed greater absorption capacity compared to ChCl/EG (3:14) and EG. Moreover, ChCl/EG (3:14) exhibited the lowest NH₃ solubility, demonstrating that the less-active component of NH₃ solubility is ChCl. ChCl/tetrazole/EG (3:7:14) demonstrated higher NH₃ capacities than EG at different pressures, indicating that tetrazole has the largest effect

on NH_3 capture. Furthermore, the capacities of NH_3 in DESs were more pronounced at low pressures. For instance, using $\text{ChCl}/\text{tetrazole}/\text{EG}$ (3:7:14), the solubility of NH_3 was five times that in EG at 0.01 MPa and 313.2 K, while its solubility in $\text{ChCl}/\text{tetrazole}/\text{EG}$ (3:7:14) was only 1.2 times that in EG at 0.1 MPa and 313.2 K.

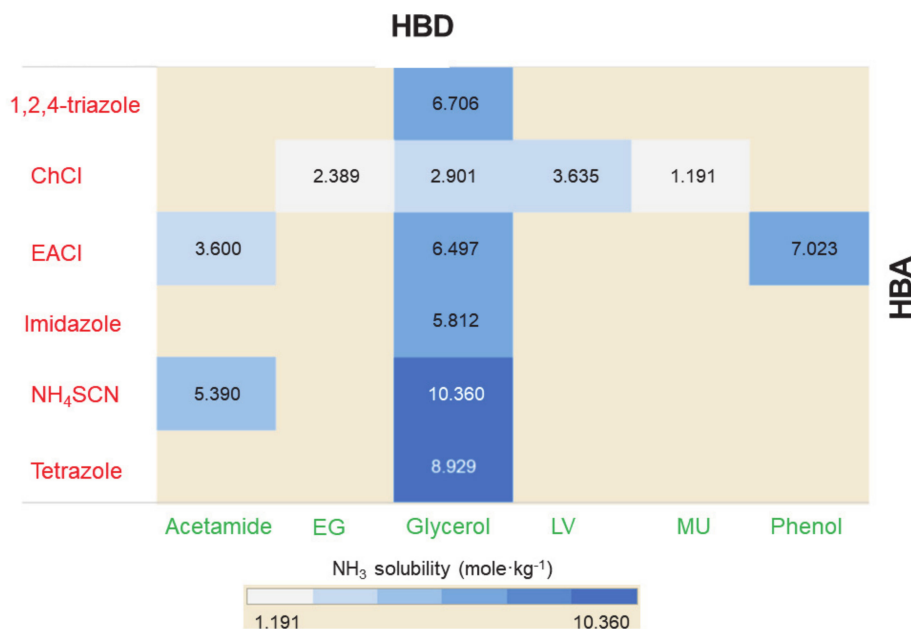


Figure 10. NH_3 solubilities in DESs based on different HBAs and HBDs at 313.2 K and around 0.1 MPa. EACI/gly, 1,2,4-triazole/gly, imidazole/gly, tetrazole/gly were mixed in 1:3 HBA:HBD molar ratio. $\text{NH}_4\text{SCN}/\text{gly}$ and $\text{NH}_4\text{SCN}/\text{urea}$ were obtained by mixing in 2:3 molar ratio. All other DESs were prepared in 1:2 molar ratio [109,111,115,116,121].

Figure 11 illustrates the effects of pressure, temperature, and DES molar ratio on the absorption capacity of NH_3 [117]. NH_3 absorption capacity increased with increasing pressure and decreasing temperature, which is a common behavior for gas absorption via liquids. However, for EACI-based DESs, as the temperature increased, the variation in NH_3 solubility steadily faded, meaning that the strength of the hydrogen bond interactions between NH_3 and EACI was negatively dependent on temperature. However, the isothermal profiles varied considerably from the ideal form, possibly because of the close interaction between EACI and NH_3 . EACI was thus the primary component in NH_3 absorption mixtures. This assessment can also be concluded by comparing NH_3 solubilities in EACI/acetamide DES mixtures with different EACI/acetamide molar ratios. EACI/acetamide 1:1 mixture had higher NH_3 solubility owing to its higher EACI content compared to 1:2 and 1:3 molar ratios. A similar behavior was observed with EACI/urea-based DESs, i.e., the absorption capacities of NH_3 decreased with increasing urea content in the EACI/urea mixtures [119]. However, for EACI/gly DESs, NH_3 solubility decreased with increasing mole fraction of EACI in the DES. The order of capacity for EACI:gly DESs molar ratios was as follows: 1:5 > 1:4 > 1:3 > 1:2. For ternary DESs, there was no clear trend for NH_3 solubility. For instance, the solubility increased (from 0.071 to 0.096 gNH_3/gDES) when the $\text{ChCl}/\text{PNA}/\text{gly}$ DES molar ratio increased from 1:3:1 to 1:3:3. However, the solubility was reduced (from 0.096 to 0.095 gNH_3/gDES) after the molar ratio was further increased from 1:3:3 to 1:3:5. Similarly, $\text{ChCl}/\text{resorcinol (RES)}/\text{gly}$ absorption capacity increased from 1:1:5 to 1:7:5 and then dropped sharply when the molar ratio was further changed to 1:9:5 [115]. This indicates that optimal mole fractions of DESs (either binary or ternary) are needed to enhance gas absorption. Furthermore, higher NH_3 solubilities were observed at lower temperatures for EACI/acetamide, EACI/urea, and EACI/gly DESs.

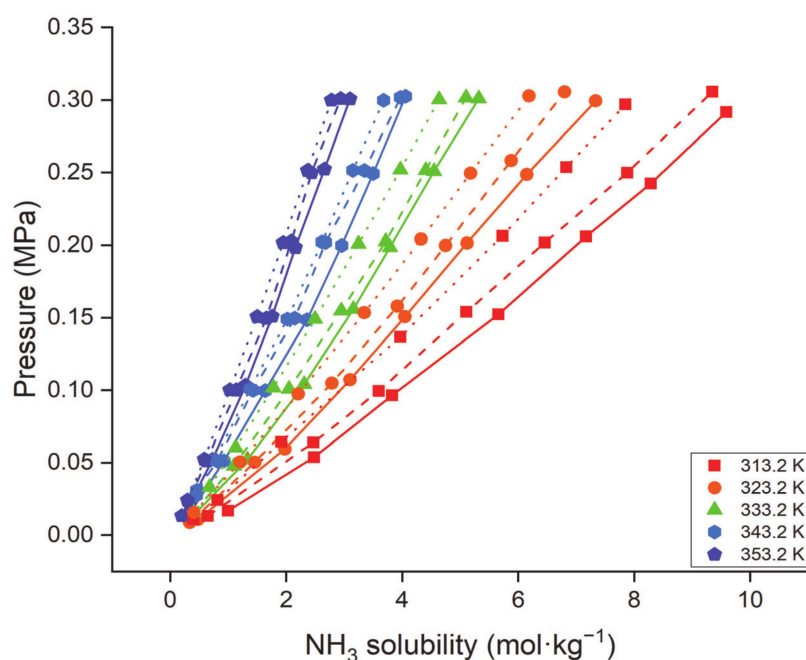


Figure 11. Effect of pressure, temperature, and molar ratio on the absorption capacity of NH₃ through EACI/acetamide based DESs; solid, dash, and dot lines indicate the 1:1, 1:2, and 1:3 EACI/acetamide molar ratios, respectively. Data are taken from [117].

The low viscosity characteristic of any solvent is favorable for the liquid transport and mass transfer of gas. The NH₃ absorption was swift (with the equilibrium time being shorter than 1.5 min) in the azole-based DESs owing to their lower viscosity (<30 mPa·s at 298.2 K) [123]. GI/acetamide (1:2) DES also exhibited fast NH₃ absorption owing to its low viscosity (21.05 mPa·s at 298.2 K), and the NH₃ pressure was drastically reduced to a constant within around 100 s [120]. NH₃ absorption capacity to achieve equilibrium was less than 60 s in EACI/phenol DESs, mainly due to their relatively low viscosities [118]. EACI/phenol DESs were prepared in different molar ratios. However, there was no significant difference between the NH₃ solubility because there were minimal viscosity changes. Similarly, ternary DESs ChCl:tetrazole:EG (3:7:14) also resulted in very fast NH₃ absorption (equilibrium time was less than 1.5 min) due to the low viscosity of DES (27.4 mPa·s at 298.2 K) [123].

3.3. H₂S Capture

Liu et al. [124] found that H₂S absorption capacity increased with increasing molar ratio of ChCl/urea DES from 1:1.5 to 1:2.5 at a fixed temperature and pressure. Furthermore, the absorption capacity of H₂S in ChCl/urea DESs was decreased linearly by increasing the temperature. Carboxylic acid-based DESs showed higher solubility compared to ChCl/urea DESs [125]. For instance, the absorption capacity of H₂S in ChCl/urea (1:2) is 0.38 (mole H₂S/kg DES) at 313.2 K and 0.2 MPa, while it is 0.70 (mole H₂S/kg DES) in ChCl/propionic acid (PA) (1:2) at 298 K and 0.184 MPa. The solubility of H₂S in carboxylic acid-based-DESs was ordered as follows: TBAB/PA (1:1) > TBAB/AC (1:1) > TBAB/formic acid (FA) (1:1) > ChCl/PA (1:2) > ChCl/AC (1:2) > ChCl/FA (1:2) at 298 K and around 0.5 MPa. The effect of HBA on the solubility of H₂S was also evident; i.e., for the same HBD, TBAB-based DESs showed higher H₂S solubility compared to ChCl-based DESs. The hydrogen bond strength of TBAB-based DESs is lower than that of the ChCl-based DESs, and ChCl consists of a hydroxyl group; therefore, the resulting hydrogen bonding interactions in ChCl-based DESs are more complex than those in TBAB-based DESs. Recently, supported DESs using fumed silica (supporting material) and DES as the loading substance were developed to

capture H₂S [126]. Triethylamine hydrochloride (TEAC) and cupric chloride (CuCl₂) were mixed at a 1:1 molar ratio to prepare the DES. The highest H₂S capacity of 9.97 mg/g DES was obtained at a 10% DES loading rate and 303.2 K. Furthermore, it was also found that TEAC/CuCl₂ (1:1) was more efficient as a loading substance than pure TEAC or CuCl₂.

4. Selectivity of DESs in Capturing Gases

SO₂ and CO₂ are two typical gases that coexist in the flue gas. Thus, it is more important to selectively capture SO₂ from simulated mixed gases containing both SO₂ and CO₂. Deng et al. [75] determined the SO₂/CO₂ selectivity (S) in six LV based DESs and compared the results with some ILs. Higher SO₂/CO₂ selectivities (134–199) were obtained using all six DESs than in the ILs (3–4 times higher). Therefore, LV-based DESs could be used as efficient absorbents for the selective capture of SO₂ from CO₂ in flue gas. Liu et al. [82] compared the performance of six phenol-based DESs for the selective absorption of SO₂. Selectivity of SO₂/CO₂ using the phenol-based DES were as follows: ChCl/GC (1:3) > ChCl/GC (1:4) > ChCl/GC (1:5) > ChCl/cardanol (CD) (1:3) > ChCl/CD (1:4) > ChCl/CD (1:5) at 293.15 K and 0.1 MPa. SO₂/CO₂ selectivity (258) using ChCl/GC (1:3) was even higher than that of the LV-based DESs used by Deng et al. [75]. However, cardanol-based DESs had lower selectivity than GC-based DESs because the alkyl long chains in cardanol showed that weak interactions with SO₂ and GC have clearly better capability to interact with SO₂. Evidently, the increased molar ratio of phenols (GC or CD) to ChCl in DESs resulted in the decreased SO₂/CO₂ selectivity. The similar trend was observed for PPZB/gly DESs [94]. The order of selectivity in terms of PPZB/gly molar ratio was as follows: 1:4 (S = 33.1) > 1:5 (S = 12.8) > 1:6 (S = 9.5).

In industrial streams, other gases coexist with NH₃, such as CO₂ and N₂. Therefore, it is imperative for solvents to capture NH₃ as well as to exhibit higher selectivity for NH₃ than for other gases. Li and co-authors [115] compared NH₃/CO₂ selectivity for binary and ternary DESs. ChCl/RES/gly (1:3:5) exhibited higher NH₃/CO₂ selectivity (142) than binary DES ChCl/RES (1:3) (64), indicating that the addition of glycerol to the binary DES did not increase the CO₂ solubility but contributed to a much higher NH₃ solubility. Furthermore, when resorcinol was replaced with phenol in ternary DES, lower selectivity (87) was recorded than in resorcinol-based ternary DES. When phenol was mixed with EACl in a 1:7 salt: alcohol molar ratio, better NH₃/CO₂ selectivities (S = 151–195 at 298.2–353.2 K) were demonstrated [118]. From the above discussion, it is obvious that glycerol as HBD and EACl as HBA play a significant role in the selective removal of NH₃ from CO₂. Therefore, EACl was mixed with glycerol at 1:2 molar ratio, and these exhibited excellent NH₃/CO₂ selectivities ranging from 818 to 5567 [116].

Azole-based binary and ternary DESs have also been investigated for the selective separation of NH₃ from NH₃/CO₂ mixtures. The performance of 1,2,4-triazole/gly (1:3) and imidazole/gly (1:3) DESs was compared with some other DESs in term of selectivity. 1,2,4-triazole/gly (1:3) exhibited higher selectivity (216.3) than imidazole/gly (1:3), equivalent to that of ChCl/phenol/EG (1:5:4) DES (218), but lower than that of NH₄SCN/gly (2:3) and ChCl/RES/gly (1:3:5) at 0.1 MPa and 313.2 K [113,115,121]. Azole-based ternary DES (ChCl/tetrazole/EG, 3:7:14) exhibited excellent selectivities ranging from 284–611 at 298.2–353.2 K and 0.043–0.1 MPa [123]. NH₃/CO₂ selectivity using EMIMC/1H-benzotriazole (1:2) was 198–107 at 298.2–353.2 K [127]. SO₂/CO₂ and NH₃/CO₂ selectivity data via DESs are collected in Table 4.

Table 4. Selectivity data of SO₂/CO₂ and NH₃/CO₂ using DESs.

DES	Molar Ratio	Selectivity	Refs.	DES	Molar Ratio	Selectivity	Refs.
SO ₂ /CO ₂ selectivity at 293.15 K, 0.1 MPa				NH ₃ /CO ₂ selectivity at 313.15 K, 0.1 MPa			
ACC/LV	1:3	155	[75]	1,2,4-triazole/gly	1:3	216	[109]
ChCl/LV	1:3	155		[Im][NO ₃] ¹ /EG	1:3	139	[128]
ChCl/GC	1:3	258	[82]	ChCl/Res/Gly	1:3:5	142	
	1:4	237		ChCl/Res	1:3	64	
	1:5	214		ChCl/phenol/Gly	1:3:5	87	
ChCl/CD	1:3	36.0		ChCl/phenol	1:3	54	
	1:4	30.0		ChCl/Res/EG	1:3:5	49	
	1:5	26.0		ChCl/urea	1:2	16.7	
TEAB/LV	1:3	183	[75]	ChCl/1,4-BD	1:3	74.7	[110]
TEAC/LV	1:3	199			1:4	79.1	
TBAB/LV	1:3	134		ChCl/2,3-BD	1:3	65.5	
TBAC/LV	1:3	141			1:4	52.9	
PPZB/gly	1:4	33.1	[94]	GI/AA	1:2	151 ²	[120]
	1:5	12.8			1:3	116 ²	
	1:6	9.50			1:4	972 ²	
				Imidazole/gly	1:3	37.3	[109]
				NH ₄ SCN/gly	2:3	609	

¹ imidazolium nitrate, ² at 303.15 K.

5. Desulfurization and Denitrification of Fuels

Because of limited available resources, oil refiners are presently processing crude oil with a higher content of sulfur and nitrogen compounds. The removal of sulfur and nitrogen is one of the major challenges in the fuel processing industry. Sulfur is usually found in fuels in the form of compounds such as thiophenes, mercaptans, and derivatives, which contribute to the emission of sulfur oxides during combustion. A number of studies on extraction desulphurization and denitrification using DESs have been reported to date. The extraction efficiency is dependent on the type of DESs used; therefore, the selection of suitable DESs is significant. Some important factors influencing the performance of DESs for sulfur and nitrogen removal include: molar ratio, type of HBA or HBD, and extraction temperature.

Desulfurization and denitrification are significantly affected by the HBA:HBD molar ratio. An increase in EG content in the DES results in higher extraction efficiency of nitrogen content. For example, ChCl/EG (1:3.5) exhibited higher extraction efficiency (70.9%) of pyridine compared to ChCl/EG (1:2) and ChCl/EG (1:3) [129]. Almashjary et al. [130] found that an increase in acid content in the DES increases the extraction efficiency of sulfur content. For instance, ChCl/PA exhibited higher extraction efficiency (~65%) of dibenzothiophene at 1:3 than at a 1:2 molar ratio in a single extraction stage. The extraction efficiency of thiophene, benzothiophene, and dibenzothiophene increased with increasing phenol content in the ChCl/phenol DESs. When the molar ratio of ChCl/phenol was increased from 1:2 to 1:4, the extraction efficiency increased; however, further increase in HBD content did not improve the extraction efficiency [131]. For TEAB/1,4-BD DES, the desulfurization efficiencies were reduced when the molar ratio was increased from 1:4 to 1:8 at the same temperature [132]. Sudhir et al. [133] studied the effect of molar ratio of phosphonium-based DESs on the extraction efficiency of dibenzothiophene. The extraction efficiency of dibenzothiophene using MTPPB/tetraethylene glycol (TetEG) DESs

were as follows: MTPPB/TetEG (1:4) ~ MTPPB/TetEG (1:6) > MTPPB/TetEG (1:3). Both MTPPB/TetEG (1:4) and MTPPB/TetEG (1:6) exhibited almost equal extraction efficiency because it approached the saturation point of the desulfurization efficiency.

The sulfur removal efficiency is significantly dependent on the type of HBA and HBD. Li et al. [6] compared the performance of different HBA and HBDs in the DESs for the removal of sulfur. For the same HBD and molar ratio, the sequence for HBAs for sulfur removal efficiency was as follows: TBAC > TMAC > ChCl. The alkyl ammonium chloride-based DESs exhibited higher removal efficiency for benzothiophene than ChCl-based DES. The extraction sequence for HBDs was as follows: polyethylene glycol > propionate > EG > TEG > glycerol > malonic acid. Among HBDs, polyol-based DESs depicted higher extraction efficiency [extraction efficiency up to 71.06% using TBAC/PEG (1:2)]. Using acids as HBDS, the desulfurization efficiencies of some DES HBDs were as follows: *p*-toluenesulfonic acid (PTSA) > 5-sulfosalicylic acid > 4-aminosalicylic acid. A positive correlation was observed between DESs acidity and desulfurization efficiencies; i.e., DES with stronger acidity exhibits higher desulfurization capabilities [134]. Li and co-authors [135] also investigated the effect of different acidic HBDs of DES on the extraction of sulfur compounds. DESs were prepared by mixing acidic HBD with TBAB. The extraction capacity of different sulfur compounds was as follows: FA ~ AC ~ PA > oxalic acid (OA) > MA > adipic acid (AD) for thiophene; FA > PA > AC > OA > MA > AD for benzothiophene; PA > AC > OA > FA > MA > AD for dibenzothiophene. Regarding the nitrogen compound, a maximum removal efficiency of around 98.2% of carbazole was reported using ChCl/PNA (1:2) DES, while ChCl/MA (1:1) showed a very low efficiency of around 34.6% [7].

Concerning extraction temperature, studies [136–138] reported that the extraction efficiencies of sulfur content are reduced with increasing extraction temperature. A high temperature range was found to be unfavorable for the extraction of sulfur compounds using DESs. Warrag et al. [139] reported that the extraction temperature had a slight effect on the extraction efficiency of thiophene, attaining a maximum value of 30% at 313.2 K. Jha et al. [140] reported that the extraction efficiency of sulfur compounds was slightly increased with the increase in extraction temperature using diglycol-based DESs. Makoś and Boczkaj [131] studied the effect of extraction temperature on the extraction efficiency. The extraction efficiencies were found to increase with the increase in temperature from 293.2 K to 313.2 K; however, a further increase in temperature (313.2 K to 343.2 K) resulted in the reduction of extraction efficiency. Using TBAC/propionate (1:2) and TBAC/PEG (1:2) DESs, high extraction efficiency of around 71% of sulfur content was achieved, and equilibrium was reached in only 10 min. The viscosity of a solvent plays an important role in reaching equilibrium; i.e., a shorter equilibrium time would be achieved with lower solvent viscosity and higher extraction capability.

The LLE method has been widely applied for the removal of sulfur and nitrogen compounds. Hizaddin et al. [141] screened 94 DESs for potential applications in the extractive denitrification of diesel via a conductor-like screening model (COSMO-RS). The extraction efficiency of nitrogen compounds was investigated in terms of capacity, selectivity, and performance index. The screening results showed higher selectivity using ammonium-based DESs but higher capacity using phosphonium-based DESs. Moreover, DESs with amide and alcohols as HBDs resulted in higher selectivity, while DESs with carboxylic acid as the HBD exhibited higher capacity. The effect of molar ratio on the selectivity and capacity was not significant. In another study, the same group [142] compared the performance of two ammonium- and phosphonium-based DESs for the extraction of pyridine, pyrrole, indoline, and quinoline from *n*-hexadecane. Phosphonium based DES (TBPB/EG, 1:2) was found to have higher selectivity values and distribution ratio than ammonium-based DES toward nitrogen compounds. Hadj-Kali et al. [143] compared the performance of four DESs for the removal of sulfur compounds (thiophene) from *n*-heptane. The four systems are compared in a ternary diagram, as shown in Figure 12. The DES based on sulfolane (Sulf) as an HBD (TBAB/Sulf, 1:7) showed higher extraction efficiency of up to 35%.

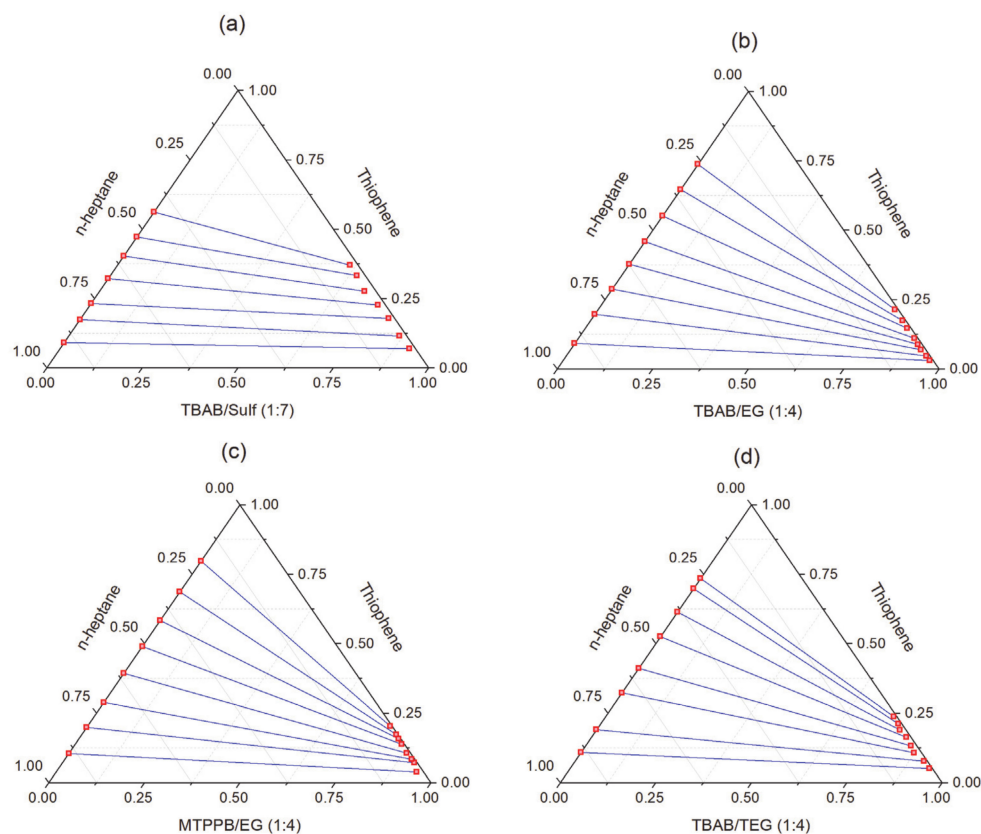


Figure 12. Experimental tie-lines for the ternary systems (a) thiophene + *n*-heptane + TBAB/Sulf (1:7), (b) thiophene + *n*-heptane + TBAB/EG (1:4), (c) thiophene + *n*-heptane + MTPPB/EG (1:4), and (d) thiophene + *n*-heptane + TBAB/TEG (1:4) at $T = 298.15$ K and 0.1 MPa. Data are taken from [143].

The extraction efficiency of sulfur compounds depends on the alkyl-chain length of the HBA; for example, the DES with longer alkyl chain length on the HBA had a higher thiophene distribution capacity. Warrag et al. [128] found very high selectivity (higher than that of ILs and DESs) for thiophene using TEAC/gly (1:2) DES but the distribution capacity was lower using the same glycerol but DESs. When glycerol was replaced with EG in the DES, higher distribution coefficient was achieved compared to glycerol-based DES owing to the higher thiophene solubility in the EG-based DES. Alli and Kroon [8] studied the LLE of a compound consisting of both sulfur and nitrogen compounds (benzothiazole) via tetrahexylammonium bromide (THAB)-based DESs. THAB/EG (1:2) exhibited a higher (greater than unity) selectivity and distribution ratio for the extraction of benzothiazole from *n*-heptane. THAB/EG (1:2) was also used for the removal of a sulfur compound (thiophene) from *n*-hexane and *n*-octane. Both selectivity and distribution ratio were lower for thiophene (compared to benzothiazole) [127]. Various DESs used for the removal of sulfur and nitrogen compounds, along with their selectivity and distribution ratio, are presented in Table 5.

Table 5. Selectivity and distribution ratio (D) for the removal of sulfur and nitrogen compounds using DESs.

DES	Mixture	S Range	D Range	Refs.
MTPPB/EG (1:4)	Benzothiazole/ <i>n</i> -hexane	9.60–40.0	2.10–3.10	[144]
MTPPB/EG (1:4)		7.00–46.8	2.10–3.50	
THAB/EG (1:2)	Benzothiazole/ <i>n</i> -heptane	7.00–27.50	2.36–3.76	[8]
THAB/gly (1:2)		7.33–35.26	1.90–2.99	

Table 5. Cont.

DES	Mixture	S Range	D Range	Refs.
TBPB/EG (1:2)	Indoline/ <i>n</i> -hexadecane	457–1,116	5.04–7.42	[142]
TBAB/EG (1:2)		833–2506	4.54–7.57	
MTPPB/gly (1:4)	Pyridine/ <i>n</i> -hexane	26.1–839.5	1.589–2.677	[145]
MTPPB/EG (1:4)		34.1–232.6	2.50–2.60	[144]
MTPPB/EG (1:4)	Pyridine/ <i>n</i> -heptane	30.1–276.9	2.60–3.40	
TBAB/EG (1:2)	Pyridine/ <i>n</i> -hexadecane	727–1228	2.93–4.39	[142]
TBPB/EG (1:2)		157–437	3.24–4.60	
Betaine/LV (1:7)	Pyrene/ <i>n</i> -decane	255.3–48,500	6.127–97.00	[146]
TBAB/EG (1:2)	Pyrrole/ <i>n</i> -hexadecane	6659–46,953	30.31–94.00	[142]
TBPB/EG (1:2)		1413–8159	27.37–98.00	
MTPPB/TEG (1:4)	Quinoline/ <i>n</i> -heptane	235.8–2327.9	4.120–9.574	[139]
TBPB/PTSA (1:1)		8644–10,866	363–467	[147]
TBPB/PTSA (1:1)	Quinoline/ <i>n</i> -pentadecane	3740–24,321	200–277	
TBAB/EG (1:2)	Quinoline/ <i>n</i> -hexadecane	3229–4955	3.56–5.00	[142]
TBPB/EG (1:2)		141–594	3.71–7.80	
TBAB/EG (1:4)	Thiophene/ <i>n</i> -heptane	8.79–30.22	0.233–0.325	[143]
MTPPB/EG (1:4)		10.12–20.19	0.251–0.373	
TBAB/TEG (1:4)		10.70–51.95	0.302–0.464	
TBAB/Sulf (1:7)		13.77–41.87	0.659–0.764	
MTPPB/TEG (1:4)	Thiophene/ <i>n</i> -heptane	20.80–161.40	0.402–0.647	[139]
THAB/EG (1:2)		1.89–9.55	0.81–0.95	[8]
THAB/gly (1:2)	Thiophene/ <i>n</i> -hexane	3.21–14.8	0.66–0.79	[148]
THAB/EG (1:2)		1.73–8.05	0.810–0.935	
THAB/EG (1:2)		2.08–11.71	0.797–0.981	
TEAC/EG (1:2)		4.81–87.99	0.320–0.512	
TEAC/gly (1:2)	Thiophene/ <i>n</i> -hexane	42.68–257.73	0.130–0.226	[149]
MTPPB/EG (1:3)		12.36–140.38	0.419–0.521	
MTPPB/gly (1:3)	Thiophene/ <i>n</i> -hexane	1.42–29.30	0.031–0.158	[148]
THAB/gly (1:2)		1.40–12.99	0.662–0.789	
THAB/gly (1:2)		1.66–17.30	0.665–0.794	
Betaine/LV (1:7)		14.4–159.7	0.396–0.489	
TEAC/EG (1:2)	Thiophene/ <i>n</i> -octane	46.95–1009.11	0.378–0.701	[150]
TEAC/gly (1:2)		137.09–794.21	0.205–0.360	
MTPPB/EG (1:3)		26.44–465.49	0.409–0.550	
MTPPB/gly (1:3)	Thiophene/ <i>n</i> -octane	107.89–673.64	0.129–0.245	

6. Conclusions

In this study, the use of DESs as green solvents for the capture of CO₂, SO_x, NO_x, and NH₃ gases was critically reviewed. We found that both components of the DESs play an important role in determining the solubility of these gases in the reported DESs. As expected, an increase in pressure and decrease in temperature increased the solubility of the gases in the DESs. However, the magnitude of enhancement varied depending on the type

of components in the DESs. The highest CO₂ absorption was in the amine-based DESs with a maximum value of 2.7 mol·kg⁻¹ for ChCl/MEA (1:7) exceeding that in aqueous MEA. However, the solubility of CO₂ depended strongly on the HBA and the range was from 0.338–2.700 mol·kg⁻¹. In addition, it was found that both physical and chemical absorption of CO₂ contribute to the solubility in amine-based DESs. The physical absorption will reduce the regeneration energy significantly. It is worth noting that not all amine based DESs had high CO₂ solubility. The presence of water in the DESs affected the solubility of CO₂ in most of the cases. Hence, it is of great importance to report the water content in DESs. Unfortunately, this was not done in many publications. It was found that the solubility of SO₂ in DESs is comparable to that in ILs with a maximum of 1.54 g SO₂/g DES for KSCN/caprolactam (1:3). For NO, the maximum solubility was 4.1 mol NO/mol DES for TBPC/DMTU (1:3) at 0.1 MPa and 303.2 K. The data for the solubility of NO₂ in DES was scarce. The maximum solubility of NO₂ was 0.551 mol NO₂/mol DES at 298.2 K in ChCl/EG (1:2). Several DESs gave promising results for the absorption of NH₃. The solubility of NH₃ in ChCl/tetrazole/EG (3:7:14), ChCl/LV (1:4), and EaCl/phenol (1:7) was 9.952, 9.494, and 9.801 mol·kg⁻¹, respectively. In all cases, the presence of water affected the solubility of gases in the DESs. It could be easily noted that a great effort is still needed to find a DES that can be used for the absorption of all acid gases discussed in this review.

Some reports indicated that the molar ratio of the components of the DES affected its ability to absorb the gases; however, other reports indicated that there are no significant changes in solubility with changes in the molar ratio. This could be attributed to the different chemical structure of the components of the DESs. Several methods, e.g., Redlich-Kwong and Peng-Robinson equation of state, were used to correlate the experimental data, and good agreement between the calculated and experimental results was achieved in most cases. Values of Henry's law constant were calculated and reported for several DESs. In addition, COSMO-RS was used to predict the solubility of CO₂ in some DESs. One important factor that was not given proper attention in the reported studies is the regeneration energy that is needed for the release of the dissolved gas from the DES. Moreover, the effect of the presence of more than one gas in the feed on the separation process must be investigated. However, it is clear that, except in the case of CO₂, more work is still needed to understand the effect of different parameters on the solubility of SO_x, NO_x, and NH₃ gases in DESs. In addition, more robust thermodynamic models for both correlating and predicting the solubility of these gases in different DESs must be tested. For CO₂, pilot plant experiments should be performed in order to move toward commercial utilization of the selected DESs in the capture of CO₂ under different operating conditions. In a parallel of this step, simulations using commercially available packages should be used to determine the optimum operational conditions of the process.

Author Contributions: Writing—original draft preparation, I.W.; Project administration, M.K.H.-K. and I.M.A.-N.; visualization, I.W.; data curation, I.W. and I.M.A.-N.; writing—review and editing, I.W., M.K.H.-K. and I.M.A.-N.; funding acquisition, M.K.H.-K.; All authors have read and agreed to the published version of the manuscript.

Funding: The authors extend their appreciation to the Deputyship for Research and Innovation, "Ministry of Education" in Saudi Arabia for funding this research work through the Project number IFKSURP-182.

Acknowledgments: The authors thank the Deanship of Scientific Research and RSSU at King Saud University for their technical support.

Conflicts of Interest: The authors declare no conflict of interest.

References

1. Sun, W.; Lin, L.C.; Peng, X.; Smit, B. Computational screening of porous metal-organic frameworks and zeolites for the removal of SO₂ and NO_x from flue gases. *AIChE J.* **2014**, *60*, 2314–2323. [[CrossRef](#)]
2. Perera, F.P. Multiple Threats to Child Health from Fossil Fuel Combustion: Impacts of Air Pollution and Climate Change. *Environ. Heal. Perspect.* **2017**, *125*, 141–148. [[CrossRef](#)]

3. Silas, K.; Ghani, W.A.W.A.K.; Choong, T.S.; Rashid, U. Carbonaceous materials modified catalysts for simultaneous SO₂/NO_x removal from flue gas: A review. *Catal. Rev.* **2019**, *61*, 134–161. [[CrossRef](#)]
4. Lemaoui, T.; Benguerba, Y.; Darwish, A.S.; Abu Hatab, F.; Warrag, S.E.; Kroon, M.C.; Alnashef, I.M. Simultaneous dearomatization, desulfurization, and denitrogenation of diesel fuels using acidic deep eutectic solvents as extractive agents: A parametric study. *Sep. Purif. Technol.* **2021**, *256*, 117861. [[CrossRef](#)]
5. Ladommatos, N.; Xiao, Z.; Zhao, H. Effects of fuels with a low aromatic content on diesel engine exhaust emissions. *Proc. Inst. Mech. Eng. Part D J. Automob. Eng.* **2000**, *214*, 779–794. [[CrossRef](#)]
6. Li, C.; Li, D.; Zou, S.; Li, Z.; Yin, J.; Wang, A.; Cui, Y.; Yao, Z.; Zhao, Q. Extraction desulfurization process of fuels with ammonium-based deep eutectic solvents. *Green Chem.* **2013**, *15*, 2793–2799. [[CrossRef](#)]
7. Ali, M.C.; Yang, Q.; Fine, A.A.; Jin, W.; Zhang, Z.; Xing, H.; Ren, Q. Efficient removal of both basic and non-basic nitrogen compounds from fuels by deep eutectic solvents. *Green Chem.* **2016**, *18*, 157–164. [[CrossRef](#)]
8. Alli, R.D.; Kroon, M.C. Extraction of benzothiazole and thiophene from their mixtures with n-heptane using tetrahexylammonium bromide-based deep eutectic solvents as extractive denitrogenation and desulfurization agents. *Fluid Phase Equilibria* **2018**, *477*, 1–11. [[CrossRef](#)]
9. Ali, H.; Khan, E. Environmental chemistry in the twenty-first century. *Environ. Chem. Lett.* **2017**, *15*, 329–346. [[CrossRef](#)]
10. Krishnan, A.; Gopinath, K.; Vo, D.-V.N.; Malolan, R.; Nagarajan, V.M.; Arun, J. Ionic liquids, deep eutectic solvents and liquid polymers as green solvents in carbon capture technologies: A review. *Environ. Chem. Lett.* **2020**, 1–24. [[CrossRef](#)]
11. Gonçalves, A.L.; Pires, J.C.; Simões, M. Green fuel production: Processes applied to microalgae. *Environ. Chem. Lett.* **2013**, *11*, 315–324. [[CrossRef](#)]
12. Xu, H.-J.; Zhang, C.-F.; Zheng, Z.-S. Selective H₂S Removal by Nonaqueous Methyl-diethanolamine Solutions in an Experimental Apparatus. *Ind. Eng. Chem. Res.* **2002**, *41*, 2953–2956. [[CrossRef](#)]
13. Song, C.; Liu, Q.; Ji, N.; Deng, S.; Zhao, J.; Li, Y.; Song, Y.; Li, H. Alternative pathways for efficient CO₂ capture by hybrid processes—A review. *Renew. Sustain. Energy Rev.* **2018**, *82*, 215–231. [[CrossRef](#)]
14. Haider, J.; Saeed, S.; Qyum, M.A.; Kazmi, B.; Ahmad, R.; Muhammad, A.; Lee, M. Simultaneous capture of acid gases from natural gas adopting ionic liquids: Challenges, recent developments, and prospects. *Renew. Sustain. Energy Rev.* **2020**, *123*, 109771. [[CrossRef](#)]
15. Lepaumier, H.; Picq, D.; Carrette, P.-L. New Amines for CO₂ Capture. I. Mechanisms of Amine Degradation in the Presence of CO₂. *Ind. Eng. Chem. Res.* **2009**, *48*, 9061–9067. [[CrossRef](#)]
16. Mirzaei, S.; Shamiri, A.; Aroua, M.K. A review of different solvents, mass transfer, and hydrodynamics for postcombustion CO₂ capture. *Rev. Chem. Eng.* **2015**, *31*, 521–561. [[CrossRef](#)]
17. Morgan, J.C.; Chinen, A.S.; Omell, B.; Bhattacharyya, D.; Tong, C.; Miller, D.C. Thermodynamic modeling and uncertainty quantification of CO₂-loaded aqueous MEA solutions. *Chem. Eng. Sci.* **2017**, *168*, 309–324. [[CrossRef](#)]
18. Kenarsari, S.D.; Yang, D.; Jiang, G.; Zhang, S.; Wang, J.; Russell, A.G.; Wei, Q.; Fan, M. Review of recent advances in carbon dioxide separation and capture. *RSC Adv.* **2013**, *3*, 22739–22773. [[CrossRef](#)]
19. Cents, A.; Brilman, D.W.F.; Versteeg, G. CO₂ absorption in carbonate/bicarbonate solutions: The Danckwerts-criterion revisited. *Chem. Eng. Sci.* **2005**, *60*, 5830–5835. [[CrossRef](#)]
20. Song, H.-J.; Park, S.; Kim, H.; Gaur, A.; Park, J.-W.; Lee, S.-J. Carbon dioxide absorption characteristics of aqueous amino acid salt solutions. *Int. J. Greenh. Gas Control.* **2012**, *11*, 64–72. [[CrossRef](#)]
21. Bernardo, P.; Clarizia, G. 30 years of membrane technology for gas separation. *Chem. Eng. Trans.* **2013**, *32*, 1999–2004.
22. Wazeer, I.; Hayyan, M.; Hadj-Kali, M.K. Deep eutectic solvents: Designer fluids for chemical processes. *J. Chem. Technol. Biotechnol.* **2018**, *93*, 945–958. [[CrossRef](#)]
23. Khandelwal, S.; Tailor, Y.K.; Kumar, M. Deep eutectic solvents (DESs) as eco-friendly and sustainable solvent/catalyst systems in organic transformations. *J. Mol. Liq.* **2016**, *215*, 345–386. [[CrossRef](#)]
24. Li, C.-J.; Chan, T.-H. *Comprehensive Organic Reactions in Aqueous Media*; Wiley: Hoboken, NJ, USA, 2007; p. 191.
25. Hyde, J.R.; Licence, P.; Carter, D.; Poliakov, M. Continuous catalytic reactions in supercritical fluids. *Appl. Catal. A Gen.* **2001**, *222*, 119–131. [[CrossRef](#)]
26. Reichardt, C.; Welton, T. *Solvents and Solvent Effects in Organic Chemistry*; Wiley: Hoboken, NJ, USA, 2010; p. 5.
27. Kerton, F.M.; Marriott, R. *Alternative Solvents for Green Chemistry*; Royal Society of Chemistry (RSC): London, UK, 2013; pp. 11–16.
28. Brennecke, J.F.; Maginn, E.J. Ionic liquids: Innovative fluids for chemical processing. *AIChE J.* **2001**, *47*, 2384–2389. [[CrossRef](#)]
29. Wang, H.; Gurau, G.; Rogers, R.D. Ionic liquid processing of cellulose. *Chem. Soc. Rev.* **2012**, *41*, 1519–1537. [[CrossRef](#)]
30. Bubalo, M.C.; Radošević, K.; Redovniković, I.R.; Halambek, J.; Srček, V.G. A brief overview of the potential environmental hazards of ionic liquids. *Ecotoxicol. Environ. Saf.* **2014**, *99*, 1–12. [[CrossRef](#)]
31. Pham, T.P.T.; Cho, C.-W.; Yun, Y.-S. Environmental fate and toxicity of ionic liquids: A review. *Water Res.* **2010**, *44*, 352–372. [[CrossRef](#)]
32. Coutinho, J.A.; Pinho, S.P. Special Issue on Deep Eutectic Solvents: A foreword. *Fluid Phase Equilibria* **2017**, *448*, 1. [[CrossRef](#)]
33. Abbott, A.P.; Capper, G.; Davies, D.L.; Rasheed, R.K.; Tambyrajah, V. Novel Solvent Properties of Choline Chloride/Urea Mixtures. *Chem. Commun.* **2003**, 70–71. [[CrossRef](#)]
34. Martins, M.A.R.; Pinho, S.P.; Coutinho, J.A.P. Insights into the Nature of Eutectic and Deep Eutectic Mixtures. *J. Solut. Chem.* **2019**, *48*, 962–982. [[CrossRef](#)]

35. Jablonský, M.; Škulcová, A.; Šima, J. Use of Deep Eutectic Solvents in Polymer Chemistry—A Review. *Molecules* **2019**, *24*, 3978. [[CrossRef](#)] [[PubMed](#)]
36. Hayyan, M.; Hashim, M.A.; Hayyan, A.; Al-Saadi, M.A.; Alnashef, I.M.; Mirghani, M.E.; Saheed, O.K. Are deep eutectic solvents benign or toxic? *Chemosphere* **2013**, *90*, 2193–2195. [[CrossRef](#)] [[PubMed](#)]
37. Hayyan, M.; Hashim, M.A.; Al-Saadi, M.A.; Hayyan, A.; Alnashef, I.M.; Mirghani, M.E. Assessment of cytotoxicity and toxicity for phosphonium-based deep eutectic solvents. *Chemosphere* **2013**, *93*, 455–459. [[CrossRef](#)]
38. Mao, S.; Li, K.; Hou, Y.; Liu, Y.; Ji, S.; Qin, H.; Lu, F. Synergistic effects of components in deep eutectic solvents relieve toxicity and improve the performance of steroid biotransformation catalyzed by *Arthrobacter simplex*. *J. Chem. Technol. Biotechnol.* **2018**, *93*, 2729–2736. [[CrossRef](#)]
39. Wen, Q.; Chen, J.-X.; Tang, Y.-L.; Wang, J.; Yang, Z. Assessing the toxicity and biodegradability of deep eutectic solvents. *Chemosphere* **2015**, *132*, 63–69. [[CrossRef](#)]
40. Radošević, K.; Bubalo, M.C.; Srček, V.G.; Grgas, D.; Dragičević, T.L.; Redovniković, I.R. Evaluation of toxicity and biodegradability of choline chloride based deep eutectic solvents. *Ecotoxicol. Environ. Saf.* **2015**, *112*, 46–53. [[CrossRef](#)]
41. Chen, Y.; Yu, D.; Lu, Y.; Li, G.; Fu, L.; Mu, T. Volatility of Deep Eutectic Solvent Choline Chloride:N-Methylacetamide at Ambient Temperature and Pressure. *Ind. Eng. Chem. Res.* **2019**, *58*, 7308–7317. [[CrossRef](#)]
42. Chen, Y.; Wang, Q.; Liu, Z.; Li, Z.; Chen, W.; Zhou, L.; Qin, J.; Meng, Y.; Mu, T. Vaporization enthalpy, long-term evaporation and evaporation mechanism of polyethylene glycol-based deep eutectic solvents. *New J. Chem.* **2020**, *44*, 9493–9501. [[CrossRef](#)]
43. Ali, E.; Hadj-Kali, M.K.; Mulyono, S.; Alnashef, I.M.; Fakeeha, A.; Mjalli, F.S.; Hayyan, A. Solubility of CO₂ in deep eutectic solvents: Experiments and modelling using the Peng–Robinson equation of state. *Chem. Eng. Res. Des.* **2014**, *92*, 1898–1906. [[CrossRef](#)]
44. Mulyono, S.; Hizaddin, H.F.; Alnashef, I.M.; Hashim, M.A.; Fakeeha, A.H.; Hadj-Kali, M.K. Separation of BTEX aromatics from n-octane using a (tetrabutylammonium bromide + sulfolane) deep eutectic solvent—Experiments and COSMO-RS prediction. *RSC Adv.* **2014**, *4*, 17597–17606. [[CrossRef](#)]
45. García, G.; Aparicio, S.; Ullah, R.; Atilhan, M. Deep Eutectic Solvents: Physicochemical Properties and Gas Separation Applications. *Energy Fuels* **2015**, *29*, 2616–2644. [[CrossRef](#)]
46. Sarmad, S.; Mikkola, J.-P.; Ji, X. Carbon Dioxide Capture with Ionic Liquids and Deep Eutectic Solvents: A New Generation of Sorbents. *ChemSusChem* **2017**, *10*, 324–352. [[CrossRef](#)] [[PubMed](#)]
47. Aissaoui, T.; Alnashef, I.M.; Qureshi, U.A.; Benguerba, Y. Potential applications of deep eutectic solvents in natural gas sweetening for CO₂ capture. *Rev. Chem. Eng.* **2017**, *33*, 523–550. [[CrossRef](#)]
48. Smith, E.L.; Abbott, A.P.; Ryder, K.S. Deep Eutectic Solvents (DESs) and Their Applications. *Chem. Rev.* **2014**, *114*, 11060–11082. [[CrossRef](#)]
49. Chen, Y.; Han, X.; Liu, Z.; Yu, D.; Guo, W.; Mu, T. Capture of Toxic Gases by Deep Eutectic Solvents. *ACS Sustain. Chem. Eng.* **2020**, *8*, 5410–5430. [[CrossRef](#)]
50. Emami, S.; Shayanfar, A. Deep eutectic solvents for pharmaceutical formulation and drug delivery applications. *Pharm. Dev. Technol.* **2020**, 1–18. [[CrossRef](#)]
51. Devries, N. *CO₂ Absorption into Concentrated Carbonate Solutions with Promoters at Elevated Temperatures*; University of Illinois at Urbana-Champaign: Urbana, IL, USA, 2014.
52. Wu, G.; Liu, Y.; Liu, G.; Pang, X. The CO₂ Absorption in Flue Gas Using Mixed Ionic Liquids. *Molecules* **2020**, *25*, 1034. [[CrossRef](#)]
53. Xie, Y. CO₂ Separation with Ionic Liquids—From Properties to Process Simulation. Ph.D. Thesis, Luleå University of Technology, Luleå, Sweden, 2016.
54. Li, X.; Hou, M.; Han, B.; Wang, X.; Zou, L. Solubility of CO₂ in a Choline Chloride + Urea Eutectic Mixture. *J. Chem. Eng. Data* **2008**, *53*, 548–550. [[CrossRef](#)]
55. Akhmetshina, A.I.; Petukhov, A.N.; Mechergui, A.; Vorotyntsev, A.V.; Nyuchev, A.V.; Moskvichev, A.A.; Vorotyntsev, I. Evaluation of Methanesulfonate-Based Deep Eutectic Solvent for Ammonia Sorption. *J. Chem. Eng. Data* **2018**, *63*, 1896–1904. [[CrossRef](#)]
56. Li, X.; Liu, X.; Deng, D. Solubilities and Thermodynamic Properties of CO₂ in Four Azole-Based Deep Eutectic Solvents. *J. Chem. Eng. Data* **2018**, *63*, 2091–2096. [[CrossRef](#)]
57. Liu, X.; Gao, B.; Jiang, Y.; Ai, N.; Deng, D. Solubilities and Thermodynamic Properties of Carbon Dioxide in Guaiacol-Based Deep Eutectic Solvents. *J. Chem. Eng. Data* **2017**, *62*, 1448–1455. [[CrossRef](#)]
58. Deng, D.; Jiang, Y.; Liu, X.; Zhang, Z.; Ai, N. Investigation of solubilities of carbon dioxide in five levulinic acid-based deep eutectic solvents and their thermodynamic properties. *J. Chem. Thermodyn.* **2016**, *103*, 212–217. [[CrossRef](#)]
59. Altamash, T.; Nasser, M.S.; Elhamarnah, Y.; Magzoub, M.; Ullah, R.; Qiblawey, H.; Aparicio, S.; Atilhan, M. Gas solubility and rheological behavior study of betaine and alanine based natural deep eutectic solvents (NADES). *J. Mol. Liq.* **2018**, *256*, 286–295. [[CrossRef](#)]
60. Ghaedi, H.; Ayoub, M.; Sufian, S.; Shariff, A.M.; Hailegiorgis, S.M.; Khan, S.N. CO₂ capture with the help of Phosphonium-based deep eutectic solvents. *J. Mol. Liq.* **2017**, *243*, 564–571. [[CrossRef](#)]
61. Sarmad, S.; Xie, Y.; Mikkola, J.-P.; Ji, X. Screening of deep eutectic solvents (DESs) as green CO₂ sorbents: From solubility to viscosity. *New J. Chem.* **2017**, *41*, 290–301. [[CrossRef](#)]
62. Zubeir, L.F.; Van Osch, D.J.G.P.; Rocha, M.A.A.; Banat, F.; Kroon, M.C. Carbon Dioxide Solubilities in Decanoic Acid-Based Hydrophobic Deep Eutectic Solvents. *J. Chem. Eng. Data* **2018**, *63*, 913–919. [[CrossRef](#)]

63. Aldawsari, J.N.; Adeyemi, I.A.; Bessadok-Jemai, A.; Ali, E.; Alnashef, I.M.; Hadj-Kali, M.K. Polyethylene glycol-based deep eutectic solvents as a novel agent for natural gas sweetening. *PLoS ONE* **2020**, *15*, e0239493. [[CrossRef](#)]
64. Blanchard, L.A.; Gu, A.Z.; Brennecke, J.F. High-Pressure Phase Behavior of Ionic Liquid/CO₂ Systems. *J. Phys. Chem. B* **2001**, *105*, 2437–2444. [[CrossRef](#)]
65. Li, Z.; Wang, L.; Li, C.; Cui, Y.; Li, S.; Yang, G.; Shen, Y. Absorption of Carbon Dioxide Using Ethanolamine-Based Deep Eutectic Solvents. *ACS Sustain. Chem. Eng.* **2019**, *7*, 10403–10414. [[CrossRef](#)]
66. Adeyemi, I.; Abu-Zahra, M.R.; Alnashef, I. Experimental Study of the Solubility of CO₂ in Novel Amine Based Deep Eutectic Solvents. *Energy Procedia* **2017**, *105*, 1394–1400. [[CrossRef](#)]
67. Anthony, J.L.; Maginn, E.J.; Brennecke, J.F. Solubilities and Thermodynamic Properties of Gases in the Ionic Liquid 1-n-Butyl-3-methylimidazolium Hexafluorophosphate. *J. Phys. Chem. B* **2002**, *106*, 7315–7320. [[CrossRef](#)]
68. Ren, H.; Lian, S.; Wang, X.; Zhang, Y.; Duan, E. Exploiting the hydrophilic role of natural deep eutectic solvents for greening CO₂ capture. *J. Clean. Prod.* **2018**, *193*, 802–810. [[CrossRef](#)]
69. Chen, Y.; Yu, D.; Chen, W.; Fu, L.; Mu, T. Water absorption by deep eutectic solvents. *Phys. Chem. Chem. Phys.* **2019**, *21*, 2601–2610. [[CrossRef](#)]
70. Ma, C.; Sarmad, S.; Mikkola, J.-P.; Ji, X. Development of Low-Cost Deep Eutectic Solvents for CO₂ Capture. *Energy Procedia* **2017**, *142*, 3320–3325. [[CrossRef](#)]
71. Chen, J.; Li, Y.; Wang, X.; Liu, W. Application of Deep Eutectic Solvents in Food Analysis: A Review. *Molecules* **2019**, *24*, 4594. [[CrossRef](#)]
72. Trivedi, T.J.; Lee, J.H.; Lee, H.J.; Jeong, Y.K.; Choi, J.W. Deep eutectic solvents as attractive media for CO₂ capture. *Green Chem.* **2016**, *18*, 2834–2842. [[CrossRef](#)]
73. Akopyan, A.V.; Eseva, E.; Polikarpova, P.; Kedalo, A.; Vutolkina, A.; Glotov, A.P. Deep Oxidative Desulfurization of Fuels in the Presence of Brønsted Acidic Polyoxometalate-Based Ionic Liquids. *Molecules* **2020**, *25*, 536. [[CrossRef](#)]
74. Deng, D.; Liu, X.; Gao, B. Physicochemical Properties and Investigation of Azole-Based Deep Eutectic Solvents as Efficient and Reversible SO₂ Absorbents. *Ind. Eng. Chem. Res.* **2017**, *56*, 13850–13856. [[CrossRef](#)]
75. Deng, D.; Han, G.; Jiang, Y. Investigation of a deep eutectic solvent formed by levulinic acid with quaternary ammonium salt as an efficient SO₂ absorbent. *New J. Chem.* **2015**, *39*, 8158–8164. [[CrossRef](#)]
76. Zhang, K.; Ren, S.; Hou, Y.; Wu, W. Efficient absorption of SO₂ with low-partial pressures by environmentally benign functional deep eutectic solvents. *J. Hazard. Mater.* **2017**, *324*, 457–463. [[CrossRef](#)] [[PubMed](#)]
77. Zhao, T.; Liang, J.; Zhang, Y.; Wu, Y.; Hu, X. Unexpectedly efficient SO₂ capture and conversion to sulfur in novel imidazole-based deep eutectic solvents. *Chem. Commun.* **2018**, *54*, 8964–8967. [[CrossRef](#)] [[PubMed](#)]
78. Jiang, B.; Zhang, H.; Zhang, L.; Zhang, N.; Huang, Z.; Chen, Y.; Sun, Y.; Tantai, X. Novel Deep Eutectic Solvents for Highly Efficient and Reversible Absorption of SO₂ by Preorganization Strategy. *ACS Sustain. Chem. Eng.* **2019**, *7*, 8347–8357. [[CrossRef](#)]
79. Chen, Y.; Jiang, B.; Dou, H.; Zhang, L.; Tantai, X.; Sun, Y.; Zhang, H. Highly Efficient and Reversible Capture of Low Partial Pressure SO₂ by Functional Deep Eutectic Solvents. *Energy Fuels* **2018**, *32*, 10737–10744. [[CrossRef](#)]
80. Yang, D.; Hou, M.; Ning, H.; Zhang, J.; Ma, J.; Yang, G.; Han, B. Efficient SO₂ absorption by renewable choline chloride–glycerol deep eutectic solvents. *Green Chem.* **2013**, *15*, 2261–2265. [[CrossRef](#)]
81. Chen, C.-C.; Wang, C.-Y.; Huang, Y.-H. Reversible absorption of nitrogen dioxide by choline chloride-based deep eutectic solvents and their aqueous mixtures. *Chem. Eng. J.* **2021**, *405*, 126760. [[CrossRef](#)]
82. Liu, X.; Gao, B.; Deng, D. SO₂ absorption/desorption performance of renewable phenol-based deep eutectic solvents. *Sep. Sci. Technol.* **2018**, *53*, 2150–2158. [[CrossRef](#)]
83. Sun, S.; Niu, Y.; Xu, Q.; Sun, Z.; Wei, X.-H. Efficient SO₂ Absorptions by Four Kinds of Deep Eutectic Solvents Based on Choline Chloride. *Ind. Eng. Chem. Res.* **2015**, *54*, 8019–8024. [[CrossRef](#)]
84. Zhang, L.; Ma, H.; Wei, G.; Jiang, B.; Sun, Y.; Tantai, X.; Huang, Z.; Chen, Y. Efficient and Reversible Nitric Oxide Absorption by Low-Viscosity, Azole-Derived Deep Eutectic Solvents. *J. Chem. Eng. Data* **2019**, *64*, 3068–3077. [[CrossRef](#)]
85. Liu, B.; Zhao, J.; Wei, F. Characterization of caprolactam based eutectic ionic liquids and their application in SO₂ absorption. *J. Mol. Liq.* **2013**, *180*, 19–25. [[CrossRef](#)]
86. Chen, Y.; Mu, T. Conversion of CO₂ to value-added products mediated by ionic liquids. *Green Chem.* **2019**, *21*, 2544–2574. [[CrossRef](#)]
87. Li, R.; Zhao, Y.; Li, Z.; Wu, Y.; Wang, J.; Liu, Z. Choline-based ionic liquids for CO₂ capture and conversion. *Sci. China Ser. B Chem.* **2018**, *62*, 256–261. [[CrossRef](#)]
88. Cao, Y.; Chen, Y.; Sun, X.; Zhang, Z.; Mu, T. Water sorption in ionic liquids: Kinetics, mechanisms and hydrophilicity. *Phys. Chem. Chem. Phys.* **2012**, *14*, 12252–12262. [[CrossRef](#)] [[PubMed](#)]
89. Deng, D.; Zhang, C.; Deng, X.; Gong, L. Efficient Absorption of Low Partial Pressure SO₂ by 1-Ethyl-3-methylimidazolium Chloride Plus N-Formylmorpholine Deep Eutectic Solvents. *Energy Fuels* **2020**, *34*, 665–671. [[CrossRef](#)]
90. Long, G.; Yang, C.; Yang, X.; Zhao, T.; Liu, F.; Cao, J. Bisazole-Based Deep Eutectic Solvents for Efficient SO₂ Absorption and Conversion without Any Additives. *ACS Sustain. Chem. Eng.* **2020**, *8*, 2608–2613. [[CrossRef](#)]
91. Sheng, K.; Kang, Y.; Li, J.; Xu, H.; Li, D. High-Efficiency Absorption of SO₂ by a New Type of Deep Eutectic Solvents. *Energy Fuels* **2020**, *34*, 3440–3448. [[CrossRef](#)]

92. Zhang, K.; Ren, S.; Yang, X.; Hou, Y.; Wu, W.; Bao, Y. Efficient absorption of low-concentration SO₂ in simulated flue gas by functional deep eutectic solvents based on imidazole and its derivatives. *Chem. Eng. J.* **2017**, *327*, 128–134. [[CrossRef](#)]
93. Liu, B.; Wang, Y.; Wei, F.; Zhao, J. Characterization of amide–thiocyanates eutectic ionic liquids and their application in SO₂ absorption. *RSC Adv.* **2013**, *3*, 2470–2476. [[CrossRef](#)]
94. Cui, G.; Liu, J.; Lyu, S.; Wang, H.; Li, Z.; Wang, J. Efficient and Reversible SO₂ Absorption by Environmentally Friendly Task-Specific Deep Eutectic Solvents of PPZBr + Gly. *ACS Sustain. Chem. Eng.* **2019**, *7*, 14236–14246. [[CrossRef](#)]
95. Zhang, J.; Yu, L.; Gong, R.; Li, M.; Ren, H.; Duan, E. Role of Hydrophilic Ammonium-Based Deep Eutectic Solvents in SO₂ Absorption. *Energy Fuels* **2019**, *34*, 74–81. [[CrossRef](#)]
96. Sun, Y.; Wei, G.; Tantai, X.; Huang, Z.; Yang, H.; Zhang, L. Highly Efficient Nitric Oxide Absorption by Environmentally Friendly Deep Eutectic Solvents Based on 1,3-Dimethylthiourea. *Energy Fuels* **2017**, *31*, 12439–12445. [[CrossRef](#)]
97. Duan, E.; Guo, B.; Zhang, D.; Shi, L.; Sun, H.; Wang, Y. Absorption of NO and NO₂ in Caprolactam Tetrabutyl Ammonium Halide Ionic Liquids. *J. Air Waste Manag. Assoc.* **2011**, *61*, 1393–1397. [[CrossRef](#)] [[PubMed](#)]
98. Wang, C.; Zheng, J.; Cui, G.; Luo, X.; Guo, Y.; Li, H. Highly efficient SO₂ capture through tuning the interaction between anion-functionalized ionic liquids and SO₂. *Chem. Commun.* **2013**, *49*, 1166–1168. [[CrossRef](#)] [[PubMed](#)]
99. Zeng, S.; He, H.; Gao, H.; Zhang, S.; Wang, J.; Huang, Y.; Zhang, S. Improving SO₂ capture by tuning functional groups on the cation of pyridinium-based ionic liquids. *RSC Adv.* **2014**, *5*, 2470–2478. [[CrossRef](#)]
100. Wang, J.; Zeng, S.; Bai, L.; Gao, H.; Zhang, S.; Zhang, S. Novel Ether-Functionalized Pyridinium Chloride Ionic Liquids for Efficient SO₂ Capture. *Ind. Eng. Chem. Res.* **2014**, *53*, 16832–16839. [[CrossRef](#)]
101. Li, J.; Kang, Y.; Li, B.; Wang, X.; Li, D. PEG-Linked Functionalized Dicationic Ionic Liquids for Highly Efficient SO₂ Capture through Physical Absorption. *Energy Fuels* **2018**, *32*, 12703–12710. [[CrossRef](#)]
102. Yang, D.; Hou, M.; Ning, H.; Ma, J.; Kang, X.; Zhang, J.; Han, B. Reversible Capture of SO₂ through Functionalized Ionic Liquids. *ChemSusChem* **2013**, *6*, 1191–1195. [[CrossRef](#)]
103. Zeng, S.; Gao, H.; Zhang, X.; Dong, H.; Zhang, S.; Zhang, S. Efficient and reversible capture of SO₂ by pyridinium-based ionic liquids. *Chem. Eng. J.* **2014**, *251*, 248–256. [[CrossRef](#)]
104. Yang, D.; Han, Y.; Qi, H.; Wang, Y.; Dai, S. Efficient absorption of SO₂ by EmimCl-EG deep eutectic solvents. *ACS Sustain. Chem. Eng.* **2017**, *5*, 6382–6386. [[CrossRef](#)]
105. Yang, D.; Zhang, S.; Jiang, D.-E.; Dai, S. SO₂ absorption in EmimCl-TEG deep eutectic solvents. *Phys. Chem. Chem. Phys.* **2018**, *20*, 15168–15173. [[CrossRef](#)]
106. Yang, D.; Zhang, S.; Jiang, D.-E. Efficient Absorption of SO₂ by Deep Eutectic Solvents Formed by Biobased Aprotic Organic Compound Succinonitrile and 1-Ethyl-3-methylimidazolium Chloride. *ACS Sustain. Chem. Eng.* **2019**, *7*, 9086–9091. [[CrossRef](#)]
107. Sun, Y.; Gao, M.; Ren, S.; Zhang, Q.; Hou, Y.; Wu, W. Highly Efficient Absorption of NO by Amine-Based Functional Deep Eutectic Solvents. *Energy Fuels* **2019**, *34*, 690–697. [[CrossRef](#)]
108. Waite, S.L.; Li, H.; Page, A.J. NO₂ Solvation Structure in Choline Chloride Deep Eutectic Solvents—The Role of the Hydrogen Bond Donor. *J. Phys. Chem. B* **2018**, *122*, 4336–4344. [[CrossRef](#)] [[PubMed](#)]
109. Deng, D.; Duan, X.; Gao, B.; Zhang, C.; Deng, X.; Gong, L. Efficient and reversible absorption of NH₃ by functional azole–glycerol deep eutectic solvents. *New J. Chem.* **2019**, *43*, 11636–11642. [[CrossRef](#)]
110. Deng, X.; Duan, X.; Gong, L.; Deng, D. Ammonia Solubility, Density, and Viscosity of Choline Chloride–Dihydric Alcohol Deep Eutectic Solvents. *J. Chem. Eng. Data* **2020**, *65*, 4845–4854. [[CrossRef](#)]
111. Duan, X.; Gao, B.; Zhang, C.; Deng, D. Solubility and thermodynamic properties of NH₃ in choline chloride-based deep eutectic solvents. *J. Chem. Thermodyn.* **2019**, *133*, 79–84. [[CrossRef](#)]
112. Li, Z.-L.; Zhong, F.-Y.; Huang, J.-Y.; Peng, H.-L.; Huang, K. Sugar-based natural deep eutectic solvents as potential absorbents for NH₃ capture at elevated temperatures and reduced pressures. *J. Mol. Liq.* **2020**, *317*, 113992. [[CrossRef](#)]
113. Zhong, F.-Y.; Peng, H.-L.; Tao, D.-J.; Wu, P.-K.; Fan, J.-P.; Huang, K. Phenol-Based Ternary Deep Eutectic Solvents for Highly Efficient and Reversible Absorption of NH₃. *ACS Sustain. Chem. Eng.* **2019**, *7*, 3258–3266. [[CrossRef](#)]
114. Zhong, F.-Y.; Huang, K.; Peng, H.-L. Solubilities of ammonia in choline chloride plus urea at (298.2–353.2) K and (0–300) kPa. *J. Chem. Thermodyn.* **2019**, *129*, 5–11. [[CrossRef](#)]
115. Li, Y.; Ali, M.C.; Yang, Q.; Zhang, Z.; Bao, Z.; Su, B.; Xing, H.; Ren, Q. Hybrid Deep Eutectic Solvents with Flexible Hydrogen-Bonded Supramolecular Networks for Highly Efficient Uptake of NH₃. *ChemSusChem* **2017**, *10*, 3368–3377. [[CrossRef](#)]
116. Jiang, W.-J.; Zhong, F.-Y.; Liu, Y.; Huang, K. Effective and Reversible Capture of NH₃ by Ethylamine Hydrochloride Plus Glycerol Deep Eutectic Solvents. *ACS Sustain. Chem. Eng.* **2019**, *7*, 10552–10560. [[CrossRef](#)]
117. Zhang, J.-Y.; Huang, K. Densities and viscosities of, and NH₃ solubilities in deep eutectic solvents composed of ethylamine hydrochloride and acetamide. *J. Chem. Thermodyn.* **2019**, *139*, 105883. [[CrossRef](#)]
118. Jiang, W.-J.; Zhong, F.-Y.; Zhou, L.-S.; Peng, H.-L.; Fan, J.-P.; Huang, K. Chemical dual-site capture of NH₃ by unprecedentedly low-viscosity deep eutectic solvents. *Chem. Commun.* **2020**, *56*, 2399–2402. [[CrossRef](#)] [[PubMed](#)]
119. Zhang, J.-Y.; Kong, L.-Y.; Huang, K. NH₃ Solubilities and Physical Properties of Ethylamine Hydrochloride Plus Urea Deep Eutectic Solvents. *J. Chem. Eng. Data* **2019**, *64*, 3821–3830. [[CrossRef](#)]
120. Deng, D.; Deng, X.; Duan, X.; Gong, L. Protic guanidine isothiocyanate plus acetamide deep eutectic solvents with low viscosity for efficient NH₃ capture and NH₃/CO₂ separation. *J. Mol. Liq.* **2020**, 114719. [[CrossRef](#)]

121. Deng, D.; Gao, B.; Zhang, C.; Duan, X.; Cui, Y.; Ning, J. Investigation of protic NH₄SCN-based deep eutectic solvents as highly efficient and reversible NH₃ absorbents. *Chem. Eng. J.* **2019**, *358*, 936–943. [[CrossRef](#)]
122. Li, Z.-L.; Zhong, F.-Y.; Zhou, L.-S.; Tian, Z.; Huang, K. Deep Eutectic Solvents Formed by N-Methylacetamide and Heterocyclic Weak Acids for Highly Efficient and Reversible Chemical Absorption of Ammonia. *Ind. Eng. Chem. Res.* **2020**, *59*, 2060–2067. [[CrossRef](#)]
123. Zhong, F.-Y.; Zhou, L.; Shen, J.; Liu, Y.; Fan, J.-P.; Huang, K. Rational Design of Azole-Based Deep Eutectic Solvents for Highly Efficient and Reversible Capture of Ammonia. *ACS Sustain. Chem. Eng.* **2019**, *7*, 14170–14179. [[CrossRef](#)]
124. Liu, F.; Chen, W.; Mi, J.; Zhang, J.-Y.; Kan, X.; Zhong, F.-Y.; Huang, K.; Zheng, A.-M.; Jiang, L. Thermodynamic and molecular insights into the absorption of H₂S, CO₂, and CH₄ in choline chloride plus urea mixtures. *AIChE J.* **2019**, *65*, e16574. [[CrossRef](#)]
125. Wu, H.; Shen, M.; Chen, X.; Yu, G.; Abdeltawab, A.A.; Yakout, S.M. New absorbents for hydrogen sulfide: Deep eutectic solvents of tetrabutylammonium bromide/carboxylic acids and choline chloride/carboxylic acids. *Sep. Purif. Technol.* **2019**, *224*, 281–289. [[CrossRef](#)]
126. Mao, J.; Ma, Y.; Zang, L.; Xue, R.; Xiao, C.; Ji, D. Efficient Adsorption of Hydrogen Sulfide at Room Temperature Using Fumed Silica-supported Deep Eutectic Solvents. *Aerosol Air Qual. Res.* **2020**, *20*, 203–2015. [[CrossRef](#)]
127. Jiang, W.-J.; Zhang, J.-B.; Zou, Y.-T.; Peng, H.-L.; Huang, K. Manufacturing Acidities of Hydrogen-Bond Donors in Deep Eutectic Solvents for Effective and Reversible NH₃ Capture. *ACS Sustain. Chem. Eng.* **2020**, *8*, 13408–13417. [[CrossRef](#)]
128. Cao, Y.; Zhang, X.; Zeng, S.; Liu, Y.; Dong, H.; Deng, C. Protic ionic liquid-based deep eutectic solvents with multiple hydrogen bonding sites for efficient absorption of NH₃. *AIChE J.* **2020**, *66*, 16253. [[CrossRef](#)]
129. Rogošić, M.; Kučan, K.Z. Deep eutectic solvents based on choline chloride and ethylene glycol as media for extractive denitrification/desulfurization/dearomatization of motor fuels. *J. Ind. Eng. Chem.* **2019**, *72*, 87–99. [[CrossRef](#)]
130. Almashjary, K.H.; Khalid, M.; Dharaskar, S.; Jagadish, P.; Walvekar, R.; Gupta, T.C.S.M. Optimisation of extractive desulfurization using Choline Chloride-based deep eutectic solvents. *Fuel* **2018**, *234*, 1388–1400. [[CrossRef](#)]
131. Makoš, P.; Boczkaj, G. Deep eutectic solvents based highly efficient extractive desulfurization of fuels—Eco-friendly approach. *J. Mol. Liq.* **2019**, *296*, 111916. [[CrossRef](#)]
132. Lee, H.; Kang, S.; Jin, Y.; Jung, D.; Park, K.; Li, K.; Lee, J. Systematic investigation of the extractive desulfurization of fuel using deep eutectic solvents from multifarious aspects. *Fuel* **2020**, *264*, 116848. [[CrossRef](#)]
133. Sudhir, N.; Yadav, P.; Nautiyal, B.; Singh, R.; Rastogi, H.; Chauhan, H. Extractive desulfurization of fuel with methyltriphenyl phosphonium bromide- tetraethylene glycol-based eutectic solvents. *Sep. Sci. Technol.* **2020**, *55*, 554–563. [[CrossRef](#)]
134. Yin, J.; Wang, J.; Li, Z.; Li, D.; Yang, G.; Cui, Y.; Wang, A.; Li, C. Deep desulfurization of fuels based on an oxidation/extraction process with acidic deep eutectic solvents. *Green Chem.* **2015**, *17*, 4552–4559. [[CrossRef](#)]
135. Li, J.-J.; Xiao, H.; Tang, X.-D.; Zhou, M. Green Carboxylic Acid-Based Deep Eutectic Solvents as Solvents for Extractive Desulfurization. *Energy Fuels* **2016**, *30*, 5411–5418. [[CrossRef](#)]
136. Jiang, W.; Li, H.; Wang, C.; Liu, W.; Guo, T.; Liu, H.; Zhu, W.; Li, H. Synthesis of Ionic-Liquid-Based Deep Eutectic Solvents for Extractive Desulfurization of Fuel. *Energy Fuels* **2016**, *30*, 8164–8170. [[CrossRef](#)]
137. Tang, X.-D.; Zhang, Y.-F.; Li, J.-J.; Zhu, Y.-Q.; Qing, D.-Y.; Deng, Y.-X. Deep Extractive Desulfurization with Arenium Ion Deep Eutectic Solvents. *Ind. Eng. Chem. Res.* **2015**, *54*, 4625–4632. [[CrossRef](#)]
138. Wang, X.; Jiang, W.; Zhu, W.; Li, H.; Yin, S.; Chang, Y.; Li, H. A simple and cost-effective extractive desulfurization process with novel deep eutectic solvents. *RSC Adv.* **2016**, *6*, 30345–30352. [[CrossRef](#)]
139. Warrag, S.E.E.; Darwish, A.S.; AbuHatab, F.O.S.; Adeyemi, I.A.; Kroon, M.C.; Alnashef, I.M. Combined Extractive Dearomatization, Desulfurization, and Denitrogenation of Oil Fuels Using Deep Eutectic Solvents: A Parametric Study. *Ind. Eng. Chem. Res.* **2020**, *59*, 11723–11733. [[CrossRef](#)]
140. Jha, D.; Haider, M.B.; Kumar, R.; Sivagnanam, B.M. Extractive desulfurization of fuels using diglycol based deep eutectic solvents. *J. Environ. Chem. Eng.* **2020**, *8*, 104182. [[CrossRef](#)]
141. Hizaddin, H.F.; Ramalingam, A.; Hashim, M.A.; Hadj-Kali, M.K. Evaluating the Performance of Deep Eutectic Solvents for Use in Extractive Denitrification of Liquid Fuels by the Conductor-like Screening Model for Real Solvents. *J. Chem. Eng. Data* **2014**, *59*, 3470–3487. [[CrossRef](#)]
142. Hizaddin, H.F.; Hadj-Kali, M.K.; Ramalingam, A.; Hashim, M.A. Extractive denitrogenation of diesel fuel using ammonium- and phosphonium-based deep eutectic solvents. *J. Chem. Thermodyn.* **2016**, *95*, 164–173. [[CrossRef](#)]
143. Hadj-Kali, M.K.; Mulyono, S.; Hizaddin, H.F.; Wazeer, I.; El-Blidi, L.; Ali, E.; Hashim, M.A.; Alnashef, I.M. Removal of Thiophene from Mixtures with n-Heptane by Selective Extraction Using Deep Eutectic Solvents. *Ind. Eng. Chem. Res.* **2016**, *55*, 8415–8423. [[CrossRef](#)]
144. Warrag, S.E.E.; Alli, R.D.; Kroon, M.C. Liquid–Liquid Equilibrium Measurements for the Extraction of Pyridine and Benzothiazole from n-Alkanes Using Deep Eutectic Solvents. *J. Chem. Eng. Data* **2019**, *64*, 4882–4890. [[CrossRef](#)]
145. Warrag, S.E.; Darwish, A.S.; Adeyemi, I.A.; Hadj-Kali, M.K.; Kroon, M.C.; Alnashef, I. Extraction of pyridine from n-alkane mixtures using methyltriphenylphosphonium bromide-based deep eutectic solvents as extractive denitrogenation agents. *Fluid Phase Equilibria* **2020**, *517*, 112622. [[CrossRef](#)]
146. Abu Hatab, F.; Darwish, A.S.; Lemaoui, T.; Warrag, S.E.E.; Benguerba, Y.; Kroon, M.C.; Alnashef, I.M. Extraction of Thiophene, Pyridine, and Toluene from n-Decane as a Diesel Model Using Betaine-Based Natural Deep Eutectic Solvents. *J. Chem. Eng. Data* **2020**, *65*, 5443–5457. [[CrossRef](#)]

147. Kamarudin, A.F.; Hizaddin, H.F.; El-Blidi, L.; Ali, E.; Hashim, M.A.; Hadj-Kali, M.K. Performance of *p*-Toluenesulfonic Acid-Based Deep Eutectic Solvent in Denitrogenation: Computational Screening and Experimental Validation. *Molecules* **2020**, *25*, 5093. [[CrossRef](#)] [[PubMed](#)]
148. Warrag, S.E.E.; Rodriguez, N.N.R.; Nashef, I.M.; Annaland, M.M.V.S.; Siepmann, J.I.; Kroon, M.C.; Peters, C.J. Separation of Thiophene from Aliphatic Hydrocarbons Using Tetrahexylammonium-Based Deep Eutectic Solvents as Extracting Agents. *J. Chem. Eng. Data* **2017**, *62*, 2911–2919. [[CrossRef](#)]
149. Warrag, S.E.E.; Adeyemi, I.; Rodriguez, N.R.; Nashef, I.M.; Annaland, M.V.S.; Kroon, M.C.; Peters, C.C. Effect of the Type of Ammonium Salt on the Extractive Desulfurization of Fuels Using Deep Eutectic Solvents. *J. Chem. Eng. Data* **2018**, *63*, 1088–1095. [[CrossRef](#)]
150. Warrag, S.E.E.; Pototzki, C.; Rodriguez, N.R.; Annaland, M.V.S.; Kroon, M.C.; Held, C.; Sadowski, G.; Peters, C.C. Oil desulfurization using deep eutectic solvents as sustainable and economical extractants via liquid-liquid extraction: Experimental and PC-SAFT predictions. *Fluid Phase Equilibria* **2018**, *467*, 33–44. [[CrossRef](#)]